

**“RELIABILITY OF STEEL BUILDING
SUBJECTED TO BLAST LOADING”**

A Thesis

*Submitted in partial fulfillment of the requirements for the award of the
degree of*

MASTER OF TECHNOLOGY

IN

CIVIL ENGINEERING

With specialization in

STRUCTURAL ENGINEERING

Under the supervision of

**Mr. Anil Kumar
(Assistant Professor)**

By

***Saurabh Kareer
(142666)***

to



JAYPEE UNIVERSITY OF INFORMATION TECHNOLOGY

WAKNAGHAT, SOLAN – 173 234

HIMACHAL PRADESH, INDIA

June 2016

CERTIFICATE

This is to certify that the work which is being presented in the project report titled “**RELIABILITY OF STEEL BUILDING SUBJECTED TO BLAST LOADING**” in partial fulfilment of the requirements for the award of the degree of Master of Technology in Civil Engineering with specialization in Structural Engineering and submitted to the Department of Civil Engineering, Jaypee University of Information Technology, Waknaghat is an authentic record of work carried out by Mr. SAURABH KAREER (Enrolment No. 142666) during the period from July, 2015 to June, 2016 under the supervision of **Mr. Anil Kumar**, Assistant Professor, Department of Civil Engineering, Jaypee University of Information Technology, Waknaghat.

The above statement made is correct to the best of my knowledge.

Date: -

Dr. Ashok Kumar Gupta	Mr. Anil Kumar
Professor and Head of Department	Assistant Professor	External Examiner
Department of Civil Engineering	Department of Civil Engineering	
JUIT Waknaghat	JUIT Waknaghat	

ACKNOWLEDGEMENTS

Foremost, I would like to express my sincere gratitude to my advisor **Mr. Anil Kumar** for the continuous support of my thesis study, for his patience, motivation, enthusiasm, and immense knowledge. His guidance has helped me in all the time of this study and writing of this report. I could not have imagined having a better advisor and mentor for my thesis study. I would also like to thank him for lending me his precious time when I had went to him.

My special thanks are due to **Prof. Ashok Kumar Gupta**, Head of the Civil Engineering Department, for all the facilities provided.

I am also very thankful to all the faculty members of the department, for their constant encouragement during the project.

I also take the opportunity to thank all my friends who have directly or indirectly helped me in my project work.

Last but not the least I would like to thank my parents, who taught me the value of hard work by their own example.

Date:

**Saurabh Kareer
(142666)**

ABSTRACT

In recent years, explosive devices are the weapon of choices for the majority of terrorist attack that not only affect the life of human beings but also the structural resistance and physical integrity. Bomb explosion near the building can cause such an amount of pressure and produce a large amount of heat resulting a high strain loading on building and its elements. Such a high strain loading can cause catastrophic damage to the building's external and internal structural frames, collapsing of walls, blowing out large expanse of windows and shutting down of critical life safety systems. Due to such impact of this large dynamic loading, efforts have been made during the past few decades to develop methods of structural analysis and design of blast resistance structure. Since blast resistant design is the important topic of study and therefore requires the careful understanding about the blast phenomena and its effect and impact on various structural elements. In the present study, the response of steel frame building subjected to blast loading, for different standoff distances has been examined by calculating blast load manually using an empirical procedure established in the literature and applying on joints as a time history loading. The different statistical properties, like normal distribution, arithmetic mean, standard deviation, skewness and kurtosis of the charge weight and the output quantities have been studied and compared from the results obtained. The probability of failure for different values of charge weight has been computed by running the Monte Carlo Simulations. The fragility curves for the two faces of the building have been plotted for different standoff distances. It has been observed that probability of failure was lower when the blast occurs opposite the face containing column flanges than the other face. Based upon the results interpretation, it is recommended that the parking lots should not be constructed in front of the face of the building and a minimum distance from the face of the building should be kept 10 m and these should always be constructed around the corners, such that the angle of incidence of the blast load to the main structural frame of the building always remain at higher values, since this reduces the blast load significantly.

CONTENTS

<i>Chapter No.</i>	<i>Particulars</i>	<i>Page Number</i>
	List of Figures	vi
	List of Tables	viii
1.	Introduction	1-6
1.1	General	1
1.2	Blast/Explosion	2
1.3	Progressive Collapse	4
1.4	Probability of failure	5
2.	Literature Review and Objectives	7-14
2.1.	General	7
2.2	Objectives of the Project	13
2.3	Need of the Project	13
2.4	Scope of the Project	14
3.	Methodology	15-28
3.1	Blast Pressure Calculations	15
3.2	Sensitivity Analysis	22
3.3	Probability Risk Assessment	22
3.4	Uncertainty and Variability	24
3.5	Reliability of Load Resisting Systems	26
4.	Problem Definition	29-32
4.1	General	29
4.2	Modelling of the Steel Building in SAP2000 [®] and Assignment of Dead and Live Loads.	30
5.	Blast Pressure Computations	33-44
5.1	Calculating the Peak Overpressure	33
5.2	Calculation of the Peak Reflected Pressure	34
5.3	Computation of the peak pressures at the different joint of the structure resulting from an explosion	36
5.4	Variation of Peak Reflected Pressure as per Kinney and Graham	39
5.5	Observations from the Plots	43

6	Statistical Properties of Charge Weight and Output Quantities	45-49
6.1	Statistical Properties Studied	45
6.2	Face I of the Building	46
6.3	Face II of the Building	47
6.4	Discussion of the Results	49
7	Time-History Analysis of the Structure	50-54
7.1	Assigning of the Time-History Loads	50
7.2	Results of the Analysis	51
8	Probability of Failure	55-59
8.1	Probability of failure for different values of the Charge Weight	55
8.1.1	Visual Basic Application for MS-Excel	55
8.1.2	Sensitivity Analysis	55
8.1.3	Monte Carlo Simulation (MCS)	55
8.1.4	Procedure to Find the Probability of Failure	56
8.2	Probability of failure for different values of the Charge Weight (W) keeping the Standoff Distance constant at 10 m	58
8.3	Interpretation of Results	59
9	Conclusions	60-61
9.1	Conclusions	60
9.2	Scope of Further Work	61
	REFERENCES	62
	APPENDIX- A: Computation Sheet for R and α	64
	APPENDIX- B: Blast Pressure Calculation Sheets	66

LIST OF FIGURES

<i>Figure no.</i>	<i>Description</i>	<i>Page no.</i>
1.1	Blast Load on Structure	2
3.1	Variation of Pressure with Distance	16
3.2	Formation of shock front in shock wave	16
3.3	Reflected Pressure Coefficient	20
3.4	Typical Blast Pressure with Time	21
3.5	Generic Representation of Flowchart of risk based decision analysis	23
3.6	Illustrations of models and probabilistic data required for reliability analysis of blast damage to built infrastructure	27
3.7	Illustration of variability of Blast loading and system response	28
4.1	Framing Plan of the Steel Building	29
4.2	Building's first floor- Model	30
4.3	Building's first floor- With steel sections	31
4.4	Building's first floor with slab	31
4.5	Three floors of building- Model	32
4.6	Three floors of building with slab	32
	The scaled distance, standoff distance, x, y, h and angle of	
5.1	Incidence	34
5.2	The UFC 3-340-02 (2008) graphs (discretized)	35-36
5.3	Distribution of blast pressure from walls to joints	37
5.4	The face of building considered for computations	37
5.5	Plot between P_{ref} vs. R for $\alpha = 0^\circ$	39
5.6	Plot between P_{ref} vs. R for $\alpha = 15^\circ$	40
5.7	Plot between P_{ref} vs. R for $\alpha = 20^\circ$	40
5.8	Plot between P_{ref} vs. R for $\alpha = 30^\circ$	41
5.9	Plot between P_{ref} vs. R for $\alpha = 45^\circ$	41
5.10	Plot between P_{ref} vs. R for $\alpha = 60^\circ$	42
5.11	Plot between P_{ref} vs. R for $\alpha = 75^\circ$	42
5.12	Plot between P_{ref} vs. R for $\alpha = 90^\circ$	43
6.1	Plots for Charge Weight at standoff distance 5 m	46

6.2	Plots for Bending Moment at standoff distance 5 m	47
6.3	Plots for Charge Weight at standoff distance 10 m	48
6.4	Plots for Bending Moment at standoff distance 10 m	49
7.1	An example of the triangular load	50
7.2	The behaviour of full structure, under Time History Loading only	51
7.3	The behaviour of the one of the faces, under Time History Loading	52
7.4	The display plot function of joint A1	52
	Behaviour of full structure, under the combination of the DL+LL+	
7.5	Time History Loading	53
	The behaviour of the one of the faces, under the combination of the	
7.6	DL+LL+ Time History Loading	53
7.7	The display plot function of joint C4	54
8.1	Different faces of building	57
8.2	Pf vs. Charge Weight (kg) for Face I standoff distance 5 m	57
8.3	Pf vs. Charge Weight (kg) for Face II standoff distance 5 m	58
8.4	Pf vs. Charge Weight (kg) for Face I standoff distance 10 m	58
8.5	Pf vs. Charge Weight (kg) for Face II standoff distance 10 m	59

LIST OF TABLES

<i>Table Number</i>	<i>Description</i>	<i>Page Number</i>
3.1	Conversion factors for various explosives	17
4.1	Beams with Moment Resisting Connections Designated with "A"	30
4.2	Steel Profiles of Columns	30
5.1	Blast Pressure Calculation	33
5.2	The Computed Blast Load on each joint of the face	38

INTRODUCTION

1.1. General

In the past few decades terrorist attacks and threats are the growing problem all over the world that not only affects the life of human being but also the structural resistance and its physical integrity. The increase in the number of terrorist attacks especially in the last few years has shown that the effect of blast loads on buildings is a serious matter that should be taken into consideration in the design process. Although these kinds of attacks are exceptional cases, man-made disasters; blast loads are in fact dynamic loads that need to be carefully calculated just like earthquake and wind. The earthquake problem is rather old, but most of the study and knowledge on this subject has been accumulated during the past sixty years. The blast problem is rather new; information about the development in this field is made available mostly through publication of the Army Corps of Engineers, Department of Defence, public institutes and other governmental office.

Due to different accidental or intentional events, the behaviour of structural components subjected to blast loading has been the subject of considerable research effort in recent years. Conventional structures, particularly that above grade, normally are not designed to resist blast loads; and because the magnitudes of design loads are significantly lower than those produced by most explosions, conventional structures are susceptible to damage from explosions. With this in mind, developers, architects and engineers increasingly are seeking solutions for potential blast situations, to protect building occupants and the structures. Disasters such as the terrorist bombings of the U.S. embassies in Nairobi, Kenya and Dares Salaam, Tanzania in 1998, the Khobar Towers military barracks in Dhahran, Saudi Arabia in 1996, the Murrah Federal Building in Oklahoma City in 1995, and the World Trade Centre in New York in 1993 have demonstrated the need for a thorough examination of the behaviour of columns subjected to blast loads (Kirk, et al., 2005). To provide adequate protection against explosions, the design and construction of public buildings are receiving renewed attention of structural engineers. Difficulties that arise with the complexity of the problem, which involves time dependent finite deformations, high strain rates, and non-linear inelastic material behaviour, have motivated various assumptions and approximations to simplify the models.

1.2. Blast/Explosion

An explosion is a very fast chemical reaction producing transient air pressure waves called **Blast Waves**. For a ground level explosive device (such as bomb in a vehicle), the pressure wave will travel away from the source in the form of a hemispherical wave front if there is no obstruction in its path. The peak overpressure (the pressure above normal atmospheric pressure) and the duration of the overpressure vary with distance from the device. The magnitude of these parameters also depends on the explosive materials from which the bomb is made and the packaging method for the bomb. Usually the size of the bomb is given in terms of a weight of TNT. City streets confine the blast wave and prevent it from radiating hemi spherically and this tends to increase the pressures to which buildings are subjected. The blast pressure waves will also be reflected and refracted by buildings, travelling around the corners and curves of a building. Blast waves are very intrusive: they will travel down side streets and over the tops of buildings, and thus all sides of a building will be subject to overpressures. As the wave moves further from the source of the explosion, the peak overpressure drops. However, the confining effect of buildings, called '**funnelling**', and rising ground means that the pressure drops more slowly than in open ground and buildings can be at risk at what might normally be considered safe distances.

When blast waves strike directly onto the face of a building, they are **reflected** from the building. The effective pressure applied to that face of the building is magnified when this occurs.

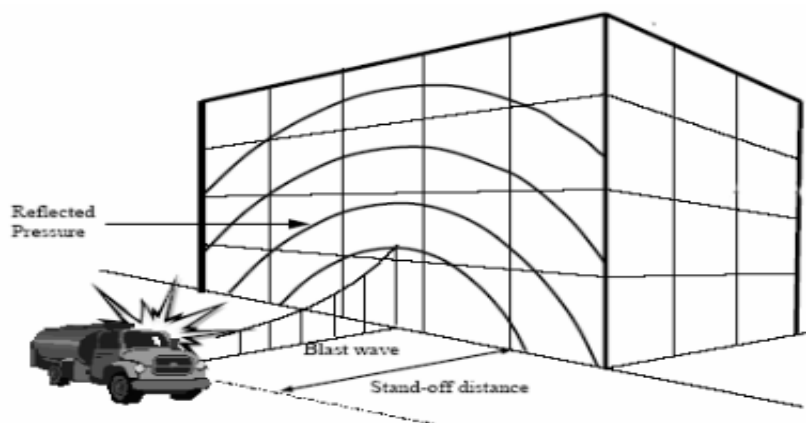


Figure 1.1 Blast Load on Structure

If a bomb is very close to a building, the building will also be impacted by shrapnel from the bomb packaging and by debris from the break-up of 'street furniture' such as litter bins and so on. This shrapnel moves at high velocity and will penetrate thin building facades and

unprotected glazing. This effect will be hazardous to personnel who should, if possible, have the chance to avail themselves of the protection offered by solid internal walls.

Explosions can be categorized on the basis of their nature as physical, nuclear and chemical events.

In physical explosion: - Energy may be released from the catastrophic failure of a cylinder of a compressed gas, volcanic eruption or even mixing of two liquid at different temperature.

In nuclear explosion: - Energy is released from the formation of different atomic nuclei by the redistribution of the protons and neutrons within the inner acting nuclei.

In chemical explosion: - The rapid oxidation of the fuel elements (carbon and hydrogen atoms) is the main source of energy.

The type of burst mainly classified as

- a. Air burst
- b. High altitude burst
- c. Under water burst
- d. Underground burst
- e. Surface burst

The discussion in this section is limited to air burst or surface burst. This information is then used to determine the dynamic loads on surface structures that are subjected to such blast pressures and to design them accordingly. It should be pointed out that surface structure cannot be protected from a direct hit by a nuclear bomb; it can however, be designed to resist the blast pressures when it is located at some distance from the point of burst.

The destructive action of nuclear weapon is much more severe than that of a conventional weapon and is due to blast or shock. In a typical air burst at an altitude below 100,000 ft. An approximate distribution of energy would consist of 50% blast and shock, 35% thermal radiation, 10% residual nuclear radiation and 5% initial nuclear radiation (J.M. Dewey,1971).

1.3. Progressive Collapse

Progressive collapse is a phenomenon in which a local damage in structure due to abnormal loads, leads to the failure of a partial or complete structural failure in such a way that the final damage is not proportional to its initial one. Abnormal loads are loads that are not considered in normal analysis of structures, but if applied, they may cause huge destructions. Although the failure of a structure is not very likely, but if occurs, it causes economical and social losses.

In past decades, there have been cases of partial or total failure of structures due to abnormal loads such as fire, impact and explosion. In the United States, Department of Defence (DoD) and General Service Administration (GSA), proposed guidelines to resist progressive collapse (DoD, 2009; GSA, 2003). Both guidelines use the Alternate Load Path (ALP) method for progressive collapse mitigation. ALP is an event independent method which does not consider the reason of the cause of an initial damage, but calculate the response of the structure after damage of one of its important load bearing elements. This method removes a middle or corner column of the structure. ALP can be used in designing new structures or to check the resistance of available structures against progressive collapse. DoD and GSA, propose Linear Static (LS), Nonlinear Static (NLS) and Nonlinear Dynamic (NLD) procedures for ALP analysis.

In NLS procedure, distributed loads according to Eq. (A) or Eq. (B) are applied to all beams:

A. $r X(DL+0.25 LL)$ (GSA load combination)

B. $r X(1.2DL+0.5 LL)+ 0.2 WL$ (DOD load combination)

where DL , LL and WL are dead, live and wind load, respectively. Factor r is a load factor to consider the dynamic effects in static analysis. Suggested values for r is two for the beams in bays adjacent to the removed column in all floors above the removed column; and is one for all other beams. In NLD method, r is equal to one for all beams. The damage criteria in NLS and NLD are suggested based on beam chord rotation and ductility.

DoD guideline defines four levels of protection for structures as follow:

- Very Low Level of Protection (VLLP),
- Low Level of Protection (LLP),
- Medium Level of Protection (MLP) and
- High Level of Protection (HLP).

In seismically compact section beams, the damage criteria for HLP and MLP are ductility of 10 and beam chord rotation of 6° .

Ductility is the ratio of ultimate displacement of column removed point to the displacement of that point at the end of its elastic stage. These damage criteria for LLP are become twice of their previous values. GSA has not defined level of protection for structures and has accepted the criteria of failure according to LLP of DoD.

Although most researches in the field of progressive collapse have been performed based on deterministic analysis using median or nominal values of design parameters (Ruth et al. 2006; Tsai and Lin,2008; Izzuddin et al., 2008-a; Izzuddin et al.,2008-b), but for more realistic analysis, it is proposed to determine uncertainty in parameters such as material and loading.

There are some methods such as Monte Carlo Simulation (MCS) technique and First Order Second Moment (FOSM) method to perform probabilistic analysis. Yield stress of steel, modulus of elasticity, dead load and live load are considered as random variables.

In structural engineering, the probability of exceeding of one parameter from a limit value is demonstrated by fragility curves, these curves are used to study the probability of progressive collapse of steel moment resisting frames. Column removed point displacement is considered as a failure criterion.

1.4. Probability of Failure

As previously mentioned, progressive collapse is happened after applying abnormal loads such as fire, impact and explosions in the structure. If each of these events are called event H , probability of progressive collapse due to event H can be calculated as the following equation:

$$P(C) = P(C|LD)P(LD|H)P(H) \quad (1.1)$$

where $P(H)$ is the probability of happening of event H , $P(LD|H)$ is the probability of local damage due to H and $P(C|LD)$ is the probability of collapse due to local initial damage. It is assumed that the probability of event H and the probability of local damage due to H is equal to 1 then only $P(C|LD)$ can be calculated. After evaluating probability of failure, fragility curves are plotted. In common structural engineering the probability of exceeding a parameter from a limit value is illustrated by **fragility curves**. Earthquake engineering uses these curves to study the

reliability of structures against earthquake. In earthquake engineering, fragility curves illustrate probability of structural failure due to seismic parameters like maximum ground acceleration. For example, to plot these curves for a structure under El-centro earthquake, the values of accelerations of this earthquake are multiplied by different factors and the response of the structure is calculated. Generally, the roof displacement of the structure is selected as reference point. By comparing these responses with limit values and using MCS method, the probability of failure is calculated. Fragility curves are the plots of probability of failure versus load factors. Fragility curves are used to study probability of progressive collapse of steel moment frames.

Literature Review and Objectives

2.1. General

The study and analysis of the blast loading on the structure started in 1960's. US Department of the Army, released a technical manual titled "structures to resist the effects of accidental explosions" in 1959. The revised edition of the manual TM 5-1300 (1990) most widely used by military and civilian organization for designing structures to prevent the propagation of explosion and to provide protection for personnel and valuable equipments. Following methods are available for prediction of blast effects on buildings structures i.e

- . • Empirical (or analytical) methods
- Semi-empirical methods
- Numerical methods

Empirical methods are essentially correlations with experimental data. Most of these approaches are limited by the extent of the underlying experimental database. The accuracy of all empirical equations diminishes as the explosive event becomes increasingly near field.

Semi-empirical methods, which are based on simplified models of physical phenomena. The attempt is to model the underlying important physical processes in a simplified way. These methods are dependent on extensive data and case study. The predictive accuracy is generally better than that provided by the empirical methods.

Numerical (or first-principle) methods are based on mathematical equations that describe the basic laws of physics governing a problem. These principles include conservation of momentum, energy, and mass.

In addition, the physical behaviour of materials is described by constitutive relationships. These models are commonly termed computational fluid dynamics (CFD) models. The key elements are the loads produced from explosive sources, how they interact with structures and the way structures respond to them. Explosive sources include gas, high explosives, nuclear and dust materials. The basic features of the explosion and blast wave phenomena are presented along with a discussion of TNT (trinitrotoluene) equivalency and Analysis of

Structural Response under Blast Loading using SAP 2000 and Autodyn blast scaling laws. The characteristics of incident overpressure loading due to atomic weapons, conventional high explosives and unconfined vapours cloud explosions are addressed and followed by a description of the other blast loading components associated with air flow and reflection process. Fertice G. has extensive study of the structures and computation of blast loading on aboveground structures

J. M. Dewey (1971) studied the properties of the blast waves obtained from the particle trajectories. First time he introduced the effect of spherical and hemispherical TNT(trinitrotoluene) in blast waves and determined the density throughout the flow by application of the Lagrangian conservation of mass equation which used for calculating the pressure assuming the adiabatic flow for each air element between the shock fronts. The temperature and the sound speed found from the pressure and density, assuming the perfect gas equation of states.

TM 5-1300 (UFC 3-340-02, 1990) is a manual titled “structures to resist the effects of accidental explosions” which provides guidance to designers, the step-to-step analysis and design procedure, including the information on such items (1) blast, fragment and shock loading. (2) principle on dynamic analysis. (3) reinforced and structural steel design and (4) a number of special design considerations.

M. V. Dharaneepathy et al. (1995) studied the effects of the stand-off distance on tall shells of different heights, carried out with a view to study the effect of distance (ground-zero distance) of charge on the blast response. An important task in blast-resistant design is to make a realistic prediction of the blast pressures. The distance of explosion from the structure is an important datum, governing the magnitude and duration of the blast loads. The distance, known as ‘critical ground-zero distance’, at which the blast response is a maximum. This critical distance should be used as design distance, instead of any other arbitrary distance.

Alexander M. Remennikov (2003) studied the methods for predicting bomb blast effects on buildings. When a single building is subjected to blast loading produced by the detonation of high explosive device. Simplified analytical techniques used for obtaining conservative estimates of the blast effects on buildings. Numerical techniques including Lagrangian, Eulerian, Euler- FCT, ALE, and finite element modelling used for accurate prediction of blast loads on commercial and public buildings.

Kirk A. Marchand et al. (2005) reviewed the contents of American Institute of Steel Construction, Inc. for facts for steel buildings give a general science of blast effects with the help of numbers of case studies of the building which are damaged due to the blast loading i.e.

Murrah Building, Oklahoma City, Khobar Towers, Dhahran, Saudi Arabia and others. Also studied the dynamic response of a steel structure to the blast loading and shows the behaviour of ductile steel column and steel connections for the blast loads.

Mark G. Stewart et al (2006) developed a probabilistic risk assessment procedure to predict risks of damage arising from blast damage to built infrastructure. They described how a probabilistic risk assessment can be used to assess and mitigate the risk of blast damage to built infrastructure, with an emphasis on structural and load-capacity systems. Such an approach can provide a rational and objective means to assess risk and decide an appropriate allocation of resources to maximize protection from blast damage. Fragility and blast reliability curves were calculated for typical window glazing. These results, in addition to threat probabilities and damage and cost data, enabled the process of assessing cost effectiveness of mitigation options to be illustrated, showing the benefits of a probabilistic risk assessment approach to decision support applications.

Quanwang Li & Bruce R. Ellingwood(2007) proposed an efficient method for selecting connections to be inspected in an existing SMRF(steel moment-resisting frame) for purposes of condition and seismic fragility assessment. It illustrated the condition assessment of two existing buildings using a probability-based connection inspection process. The benefits of an analysis-based inspection scheme based on an associated probability model of connection damage were demonstrated, and a procedure to assess the likely **performance** of un-repaired buildings in a future earthquake was developed.

Jamie Ellen Padgett, and Reginald DesRoches(2007) identified and evaluated a range of potential sources of uncertainty associated with a seismic performance assessment of portfolio(class) structures, using retrofitted MSSS steel girder bridges as a case study. The sensitivity study presented utilizes design of experiments principles to identify which modelling parameters significantly impact the seismic response of a number of different component responses in retrofitted bridges. The results of the study provide insight on the potentially uncertain modelling parameters that most significantly affect the seismic response of the retrofitted systems. The findings of this sensitivity study are extended to evaluate which sources of uncertainty actually have a significant effect on the failure estimates and fragility curves for these portfolios of structures. The relative importance of sources of uncertainty with regard to ground motion, geometry, and modeling parameters is evaluated in a comparative assessment of fragility curves developed under increasing levels of uncertainty treatment. Fragility curves developed considering only those parameters identified in the sensitivity study as important are nearly identical to those developed with all potential sources treated as variables. The fragility is found to be particularly sensitive to the propagation of

uncertainty in the base geometry (span length, column height, deck width) which is inherent to vulnerability assessments for structural portfolios. Such findings help maximize the return on efforts targeted at developing reliable fragility curves for classes of structures for use in regional seismic risk assessments.

Young and James(2008) suggested that building will have greater resistance to blast loads if it is designed for strong ground motion. Three story steel building is modelled and magnitude and distribution of blast load using computer software is estimated. For generating air blast loading, hemispherical surface of different weight and at different distance is considered. A standoff distance of greater than 15 feet should provide adequate protection against blast. Demand/capacity (D/C)ratio is used to indicate area of potential problem, when non-linear analysis is conducted. Rigid diaphragm is effective in distributing the blast load from the front fall to the other frame on the perimeter, provided that pressure does not enter to the building.

I.Zentner et al (2008) determined fragility curves for nuclear power plant equipment by means of numerical simulation accounting for random excitation due to earthquake ground motion as well as structural and model uncertainties. The unknown parameters of the fragility curve, median and logarithmic standard deviation, were estimated from the numerical experiments maximizing the corresponding likelihood function. The peak ground acceleration (or spectral acceleration) remains the preferred parameter in seismic PRA since hazard curves are established with respect to this parameter.

D. Asprone et al (2008) conducted the probabilistic analysis of progressive collapse of a typical RC structure, induced by a blast event. They presented a methodology for calculating the annual risk of collapse for a civil infrastructure structure subjected to both seismic and blast threats, using a bi-hazard approach. Given that a blast event of interest takes place, the probability of progressive collapse is calculated using a MC simulation procedure, producing set of possible realizations of the blast scenario in terms of the charge location and intensity. The simulation procedure implements an efficient plastic limit state analysis, formulated and solved as a linear programming problem, to verify whether progressive collapse mechanisms are activated under the service vertical loads or not. This leads to a significant increase in computational efficiency compared to the use of classical finite element analysis. The probability of collapse given an earthquake event of interest can be calculated by integrating the seismic fragility of the structure and the seismic hazard for the site. Once the contributions of seismic and blast threats are evaluated, they can be summed up to yield the annual risk of collapse. This study also confirms that seismic retrofit schemes can also be effective in mitigating the risk of progressive collapse due to an explosion. This result also emphasizes the

importance of considering blast criteria in the rehabilitation design of strategic structures in seismic zones.

Zeynep Koccaz et al (2008) studied the blast resistant building design theories, the enhancement of building security against the effects of explosives in both architectural and structural design process and the design techniques that should be carried out. Firstly, explosives and explosion types have been explained briefly. In addition, the general aspects of explosion process have been presented to clarify the effects of explosives on buildings. To have a better understanding of explosives and characteristics of explosions will enable us to make blast resistant building design much more efficiently. Essential techniques for increasing the capacity of a building to provide protection against explosive effects is discussed both with an architectural and structural approach.

Wibowo and Lau(2009) presented a brief overview of progressive collapse phenomenon in structures. They discussed the approaches of several code and standard provisions on preventing progressive collapse and the merits and limitations of available analysis methods for assessment of progressive collapse of structures. The significance of seismic load effects in progressive collapse behaviour of structures had also been discussed. It is concluded that seismic progressive collapse of structures can be analyzed by modifying the current analysis procedures.

Jinkoo Kim & Taewan Kim(2009) concluded that the load resisting capacity increased as the number of storeys and the number of spans increases but if the length of the span is increased, the load resisting capacity against progressive collapse decreases. These results when compared with incremental nonlinear dynamic analysis depicts that the maximum load factors resulted from the dynamic analysis were a little less than those from push down analysis. As the number of bays and design earthquake load increases, the resistance to progressive collapse also increases.

Mehrdad et al.(2011) studied the Progressive collapse Resistance of an Actual 11- Storey Structure Subjected to severe Initial Damage. They investigated the progressive collapse resistance of the Crowne Plaza Hotel, an 11-story aboveground structure in Houston, Texas, that was constructed in 1973. The experimental study depicts that the initial damage was caused by simultaneous explosion of four first floor neighbouring columns and two second floor perimeter deep beam segments. The structure resisted progressive collapse with a maximum permanent vertical displacement at the top of the exploded columns of only about 56 mm. The progressive collapse resistance of the structure is significantly affected by the axial compressive force developing in beam. The beam axial compressive force enhances its

flexural strength and in turns its resistance to progressive collapse. Two analytical models were developed out of which one includes only flexural degrees of freedom and other includes both flexural and axial deformations.

Arash Naji and Fereidoon Irani(2012) performed sensitivity analysis to study the effect of uncertainty of dead and live loads, and properties of steel such as modulus of elasticity and yield stress of steel on the response of column removed point. Then fragility curves were also plotted to investigate the probability of progressive collapse of steel moment frames. Finally, Monte Carlo simulation (MCS) and First Order Second Moment (FOSM) method were used to create probability distribution function of failure.

Manmohan Dass Goel et al(2012) presented various empirical relations available for computation of blast load in the form of pressure-time function resulting from the explosion in the air. Different empirical techniques available in the form of charts and equations were reviewed first and then the various blast wave parameters were computed using these equations. This paper provided various blast computation equations, charts, and references in a concise form at a single place and to serve as base for researchers and designers to understand, compare, and then compute the blast wave parameters. The main parameters describing blast wave positive phase, i.e. peak positive over pressure (P_{pos}), positive duration (t_{pos}), and impulse (I) can be computed using the Kinney and Grahm's equations. The negative phase parameters, i.e. under pressure (P_{neg}) and negative duration (t_{neg}) can be computed using Krauthammer and Altenberg equations. The wave decay parameter (b) can be computed using equation presented by Teich and Gebekken. Moreover, the under pressure pulse and the time at which maximum negative pressure occurs can be computed using the equation proposed by Teich and Gebekken. Thus, by using the above mentioned equations whole description of the blast wave can be achieved.

Tavakoli and Kiakogouri (2013) investigated the progressive failure using alternate load method and non – linear Dynamic analysis. They studied the structural response of building under sudden loss of column with or without external blast loading. Results shows that the progressive collapse is dependent on location of column loss. Non-linear dynamic analysis provides larger structural response than linear dynamic analysis. According to the results, the standoff distance is very sensitive in structural responses. So increasing distance with reduce the structural damage.

S.Jeyarajan et al (2015) investigated the robustness of steel-concrete composite frames under sudden column loss. Various lateral load resisting systems, including composite slab and joint contributions were taken into account in progressive collapse analysis. Ten-storey

steel buildings with (1) diagonal braces at corners (2) centre core wall (3) rigid moment joints were investigated for corner, perimeter and internal column loss. The investigations concluded that simple braced frames are more susceptible to the progressive collapse compare to the moment resisting frames which has higher redundancy to redistribute the loads. Various framing schemes and joint types are investigated to improve the robustness of the simple braced frames. End-plate beam-to-column joint is proposed instead of fin plate joint due to greater initial rotational stiffness and moment resistance. Vierendeel truss may be introduced at certain floor level (e.g. mechanical floor) in a multi-storey building to improve the robustness against the loss of critical column. This system can be used not only for new design but also for retrofitting of existing building, since only the affected floor needed to be modified by converting the simple joints to rigid moment joints. In addition, modified fin plate joint with added plate stiffener is proposed for column-to-beam joint to improve the robustness of simple frame.

2.2. Objectives of the Project

1. To compute the blast loading on a moment resisting steel frame using empirical relationships.
2. To estimate the Progressive Collapse Potential of moment resisting steel frame subjected to blast load.
3. To perform reliability analysis using the fragility curves for the above building for a number of scenarios

2.3. Need of the Project

There is a rising threat in the world, due to an increase in global terrorism. This creates an increased danger to critical infrastructure. Buildings are critical to society due to their importance as centres of government, business, education and residence. Some buildings are important to society as a whole due to the type and importance of the work done in them, and the symbolic nature of the structures. Events which can damage these structures, such as earthquakes, extreme winds, blasts, can result in downtime for the buildings operations which, due to their importance, would create a negative impact on society.

To minimize the potential impact of these terrorist attacks, a systematic approach to assess the causes and outcomes of those events is required. Thus the estimation of the resiliency via structural design and post-event analysis by determining the building damage can assist in planning future use of the structure post-attack.

2.4. Scope of the Project

In order to achieve the above-mentioned objectives the following things need to be carried out:

- All computations for dynamic loading on the steel structure to evaluate the blast pressure using Kinney and Graham's approach.
- Computation of the blast loads on the structural joints from peak reflected pressure.
- Plotting of the fragility curves for various scenarios.

3.1. Blast Pressure Calculations

Before progressing towards the calculations of the blast loads the following terms should be considered: (as per IS 4991:1968)

1. Stand-off distance: It is the distance between the bomb and the building.
2. Blast Wind - It is the moving air mass along with the over-pressures resulting from pressure difference behind the shock wave front. The blast wind movement during the positive phase of the overpressures is in the direction of shock front propagation.
3. Clearance Time - This is the time in which the reflected pressure decays down to the sum of the side on overpressure and the drag pressure.
4. Decay Parameter - It is the coefficient of the negative power of exponent e governing the fall of pressure with time in the pressure-time curves.
5. Drag Force - It is the force on a structure or structural element due to the blast wind. On any structural element, the drag force equals dynamic pressure multiplied by the drag coefficient of the element.
6. Ductility Ratio --It is the ratio of the maximum deflection to the deflection corresponding to the elastic limit.
7. Dynamic Pressure- It is the pressure effect of air mass movement called the blast wind.
8. Equivalent Bare Charge - It is the weight of a bare high explosive charge geometrically similar to any given cased charge, which produces the same blast field as the given cased charge.
9. Ground Zero - It is the point on the earth surface vertically below the explosion.
10. Impulse - Impulse per unit of projected area is the pressure-time product given by the area under the pressure-time curve considered for the positive phase only unless otherwise specified.
11. Mach Number - It is the ratio of the speed of the shock front propagation to the speed of sound in standard atmosphere at sea level.

12. Overpressure - It is the rise in pressure above atmospheric pressure due to the shock wave from an air blast.
13. Reflected Overpressure - It is the overpressure resulting due to reflection of a shock wave front striking any surface. If the shock front is parallel to the surface, the reflection is normal.
14. Shock Wave Front-It is the discontinuity between the blast wave and the surrounding atmosphere. It propagates away from the point of explosion in all directions at a speed greater than the speed of sound in the undisturbed atmosphere.
15. Side-on Overpressure -It is the overpressure if it is not reflected by any surface.
16. Transit Time - It is the time required for the shock front to travel across the structure or its element under consideration.
17. Yield -It is a measure of the size of the explosion expressed in equivalent weight of reference explosive.

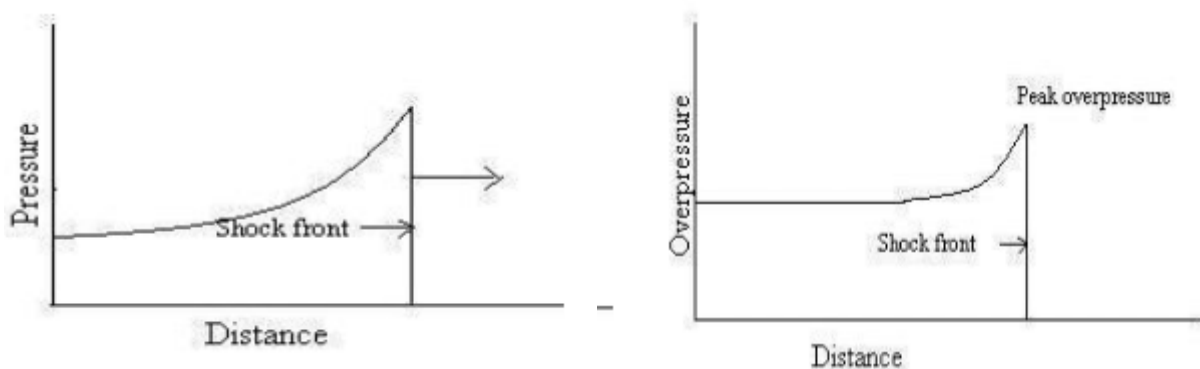


Figure 3.1 Variation of Pressure with Distance **Figure.3.2 Formation of shock front in shock wave**

Conventional buildings are constructed quite differently than hardened military structures and as such are generally quite vulnerable to blast and ballistic threats. In order to design structures which are able to withstand explosions it is necessary to first **quantify** the effects of such explosions.

I. Converting Charge Mass Into Equivalent TNT Mass

Use of the TNT (Trinitrotoluene) as a reference for determining the scaled distance, Z , is universal. The first step in quantifying the explosive wave from a source other than the TNT, is to convert the charge mass into an equivalent mass of the TNT to be considered. It is performed so that the charge mass of explosive is multiplied by the conversion factor based on the specific energy of the charge and the TNT. Specific energy of different explosive types and their conversion factors to that of the TNT are given as:

Table 3.1 Conversion factors for various explosives

EXPLOSIVE	SPECIFIC ENERGY Q _x kJ/kg	TNT EQUIVALENT Q _x /Q _{TNT}
Compound B (60% RDX, 40% TNT)	5190	1.148
RDX(Ciklonit)	5360	1.185
HMX	5680	1.256
Nitro- glycerine(liquid)	6700	1.481
TNT	4520	1.00
Explosive gelatine	4520	1.00
60% nitro- glycerine(dynamite)	2710	0.600
Semtex	5660	1.250
C4	6057	1.340

II. Scaled distance

All blast parameters are primarily dependent on the amount of energy released by a detonation in the form of a blast wave and the distance from the explosion. A universal normalized description of the blast effects can be given by scaling distance relative to $(E/P_0)^{1/3}$ and scaling pressure relative to P_0 , where E is the energy release (kJ) and P_0 the ambient pressure (typically 100 kN/m²). For convenience, however, it is general practice to express the basic explosive input or charge weight W as an equivalent mass of TNT.

Results are then given as a function of the dimensional distance parameter. Scaling laws provide parametric correlations between a particular explosion and a standard charge of the same substance.

$$\text{Scaled Distance } (Z) = \frac{R}{\sqrt[3]{W}} \quad (3.1)$$

Where, R is the actual effective distance (in m) from the explosion and W is generally expressed in pounds or kilograms.

III. Determination of Blast Pressure

- a. **PEAK INCIDENT PRESSURE:** The sudden increased value of the pressure on the surface due to an explosion resulting at a distance from the surface parallel to the propagation of the blast wave is called as the peak incident pressure.

The estimations of peak overpressure due to spherical blast based on scaled distance

$Z = \frac{R}{\sqrt[3]{W}}$ was introduced by Brode:

$$P_{\text{pos}} = \frac{6.7}{Z^3} + 1 \text{ bar} \quad (P_{\text{pos}} > 10 \text{ bar}) \quad (3.2)$$

$$P_{\text{pos}} = \frac{0.975}{Z} + \frac{1.455}{Z^2} + \frac{5.85}{Z^3} - 0.019 \text{ bar} \quad (0.1 < P_{\text{pos}} < 10 \text{ bar}) \quad (3.3)$$

In 1961, Newmark introduced a relationship to calculate the maximum blast pressure (P_{SO}), in bars, for a high explosive charge detonates at the ground surface as:

$$P_{\text{pos}} = 6784 \frac{W}{R^3} + 93 \left(\frac{W}{R^3} \right)^{1/2} \quad (3.4)$$

In 1987, Mills introduces another expression of the peak overpressure in kPa, in which W is the equivalent charge weight in kilograms of TNT and Z is the scaled distance.

$$P_{\text{pos}} = \frac{1772}{Z^3} + \frac{114}{Z^2} + \frac{108}{Z} \quad (3.5)$$

Other than these, Kinney and Grahm (1985) presented the following equation to compute the peak positive overpressure based on the analysis of large experimental data:

$$P_{\text{POS}} = P_0 \frac{808 \left[1 + \left(\frac{Z}{4.5} \right)^2 \right]}{\sqrt{\left[1 + \left(\frac{Z}{0.048} \right)^2 \right]} \times \sqrt{\left[1 + \left(\frac{Z}{0.32} \right)^2 \right]} \times \sqrt{\left[1 + \left(\frac{Z}{1.35} \right)^2 \right]}} \quad (\text{bar}) \quad (3.6)$$

- b. POSITIVE TIME DURATION (t_{pos}) :The time difference between passing of a wave front and the end of the positive pressure phase marked by the passing of zero pressure point at a particular surface is called as the positive time duration of the blast wave. The positive time duration of a blast wave on any surface depends on the dissipation of the waves around that surface. If the surface is of small size, the positive time duration will be less as compared to a larger surface as the time required to surpass the surface will be more, hence, less dissipation possible.

Kinney and Graham (1985) presented the following relation for the positive time duration:

$$t_{pos} = W^{1/3} \frac{980 \left[1 + \left(\frac{Z}{0.45} \right)^{10} \right]}{\left[1 + \left(\frac{Z}{0.02} \right)^3 \times \left[1 + \left(\frac{Z}{0.74} \right)^6 \right] \right] \times \sqrt{\left[1 + \left(\frac{Z}{6.9} \right)^2 \right]}} \text{ (msec)} \quad (3.7)$$

- c. POSITIVE IMPULSE (I_{pos}) :The area under the pressure-time history curve is called as impulse. The peak pressure decreases rapidly from the highest value to zero, described as quasi-exponential decrease. For simplicity, this decrease in the value of the peak pressure can be considered as triangular, rectangular keeping the impulse constant. Kinney and Graham (1985) presented the following relation for positive impulse:

$$I_{pos} = \frac{0.067 \sqrt{\left[1 + \left(\frac{Z}{0.23} \right)^4 \right]}}{Z^2 \sqrt[3]{1 + \left(\frac{Z}{1.55} \right)^2}} \text{ bar-ms} \quad (3.8)$$

- d. PEAK REFLECTED PRESSURE:

When a pressure wave generated from an explosion impinge a surface at an angle, it is reflected, which results in higher pressure on the surface than the incident side-on pressure. The magnitude of the reflected pressure depends on the angle of incidence of the blast wave, the radial distance of the detonation point from the surface, peak incident pressure developed due to the explosion, the type of pressure wave, and the

properties of the surface. The magnitude of the reflected pressure is generally determined from the coefficient of reflection,

$$P_{ref} = C_r P_{pos} \quad (3.9)$$

Where

C_r = coefficient of reflection

UFC 3-340-02 gives the detailed procedure of determining the peak reflected pressure on a surface depending upon the peak incident pressure and angle of incidence of the waves. Figure shows the coefficient of reflection based on the peak incident pressure of the explosion and the angle of incidence of the blast wave at a particular point on the surface.

The angle of incidence varies from 0° (wave parallel to the surface) to 90° (wave perpendicular to the surface) with the peak incident pressure.

A full discussion and extensive charts for predicting blast pressures and blast durations are given by Mays and Smith and UFC 3-340-02 (2008).

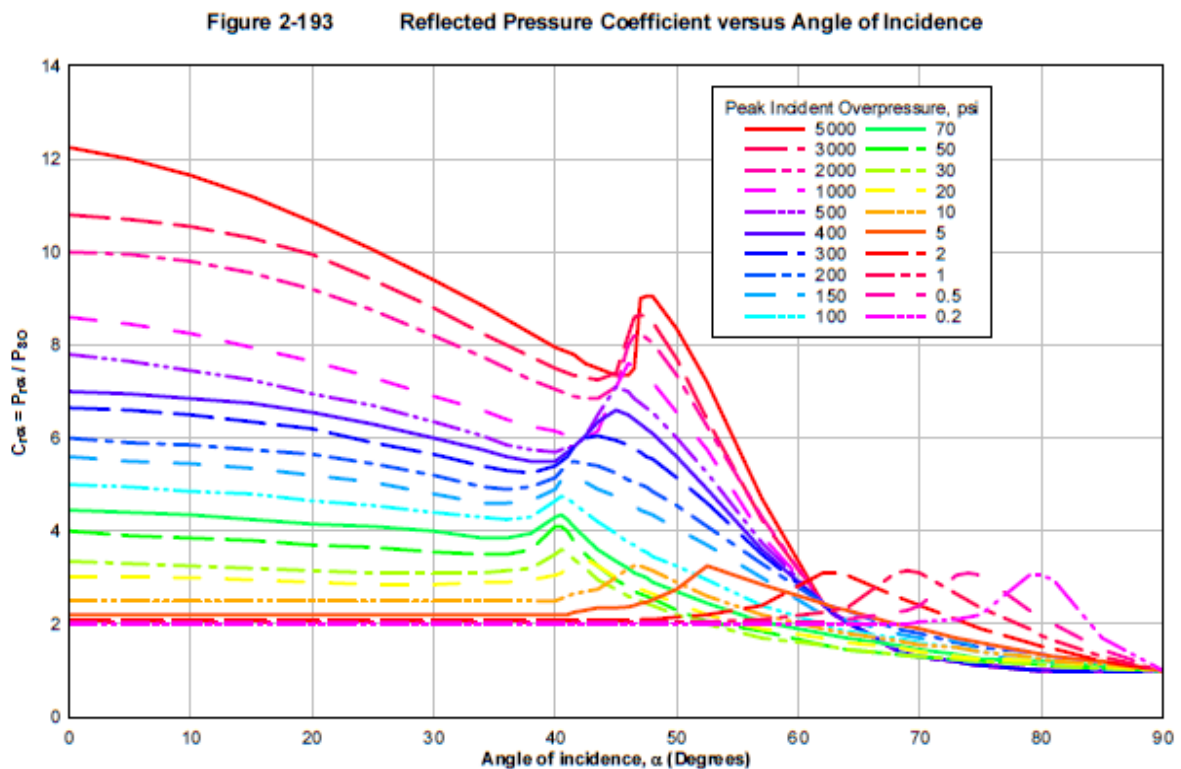


Figure 3.3 Reflected Pressure Coefficients

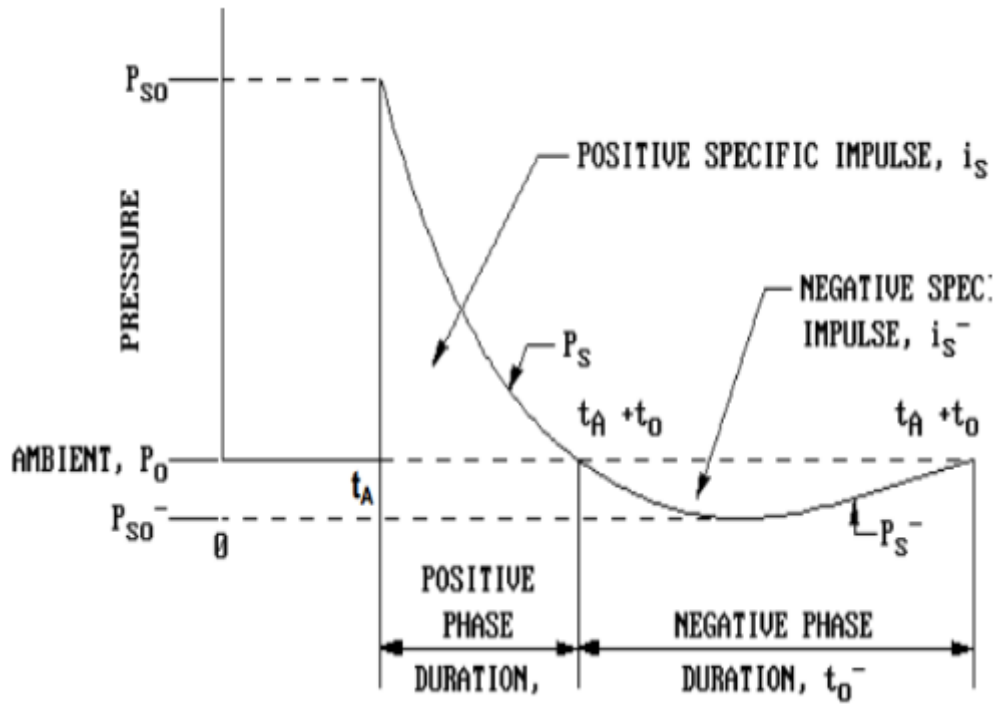


Figure 3.4 Typical Blast Pressure with Time.

WHERE

P_r = Peak Reflected Overpressure

P_{pos} = Peak Static Pressure

i_r = Impact due to reflected overpressure

i_s = Impact due to static pressure

t_A = Arrival time

t_o = Positive phase duration

U = Blast wave velocity

L_w = Length of Blast wave

For design purposes, reflected overpressure can be idealized by an equivalent triangular pulse of maximum peak pressure P_r and time duration t_d , which yields the reflected impulse (i_r).

$$\text{Reflected Impulse } (i_r) = \frac{1}{2} P_r t_d \quad (3.10)$$

Duration t_d is related directly to the time taken for the overpressure to be dissipated.

3.2. Sensitivity Analysis

Before performing probabilistic analysis, sensitivity analysis should be done to find out how much the responses are sensitive to design and applied load parameters. Three different methods to perform sensitivity analysis are used:

- First Order Second Moment (FOSM) method,
- Monte Carlo Simulation (MCS) and
- Tornado Diagrams (TD).

Monte Carlo Simulation (MCS)

Sensitivity analysis may also be performed by MCS method (Shudler, 1997). In this method, it is necessary to know the probability density function of all random variables at the beginning of process. For large number of variables, MCS is more convenient (Bucher, 1988). MCS method can be used to verify other proposed methods (Lee and Mosalam, 2006). In MCS, random variables should be generated with their mean and standard deviation.

3.3. Probability Risk Assessment

A probabilistic risk assessment procedure is developed to predict risks of damage arising from blast damage to built infrastructure. In performing a risk analysis, a number of steps are basic to the analysis and independent of the system being considered. Fig. 3 illustrates a flowchart for risk-based decisions, which is consistent with the Australian and New Zealand Risk Management Code AS/NZS 4360 Standards Australia 2004. A general description of probabilistic risk analysis and assessments for engineering systems is provided by Stewart and Melchers (1997) and Faber and Stewart (2003). Clearly, if there is 100% certainty of information and outcomes, then the probability of failure is either 0.0 or 1.0. However, this is seldom the case:

- Input data: expert predictions, material strengths, explosive weight, stand-off distance, structural condition, etc.;
- Accuracy of predictive models: computer models, threat scenarios, consequence models, etc.;
- and
- Inherent variability: weather, individual exposure to hazard, time of blast, etc.

This all leads to uncertainties associated with the magnitude of a blast, its likelihood, and the consequences. A PRA propagates these uncertainties through the computations to reveal an estimate of risk.

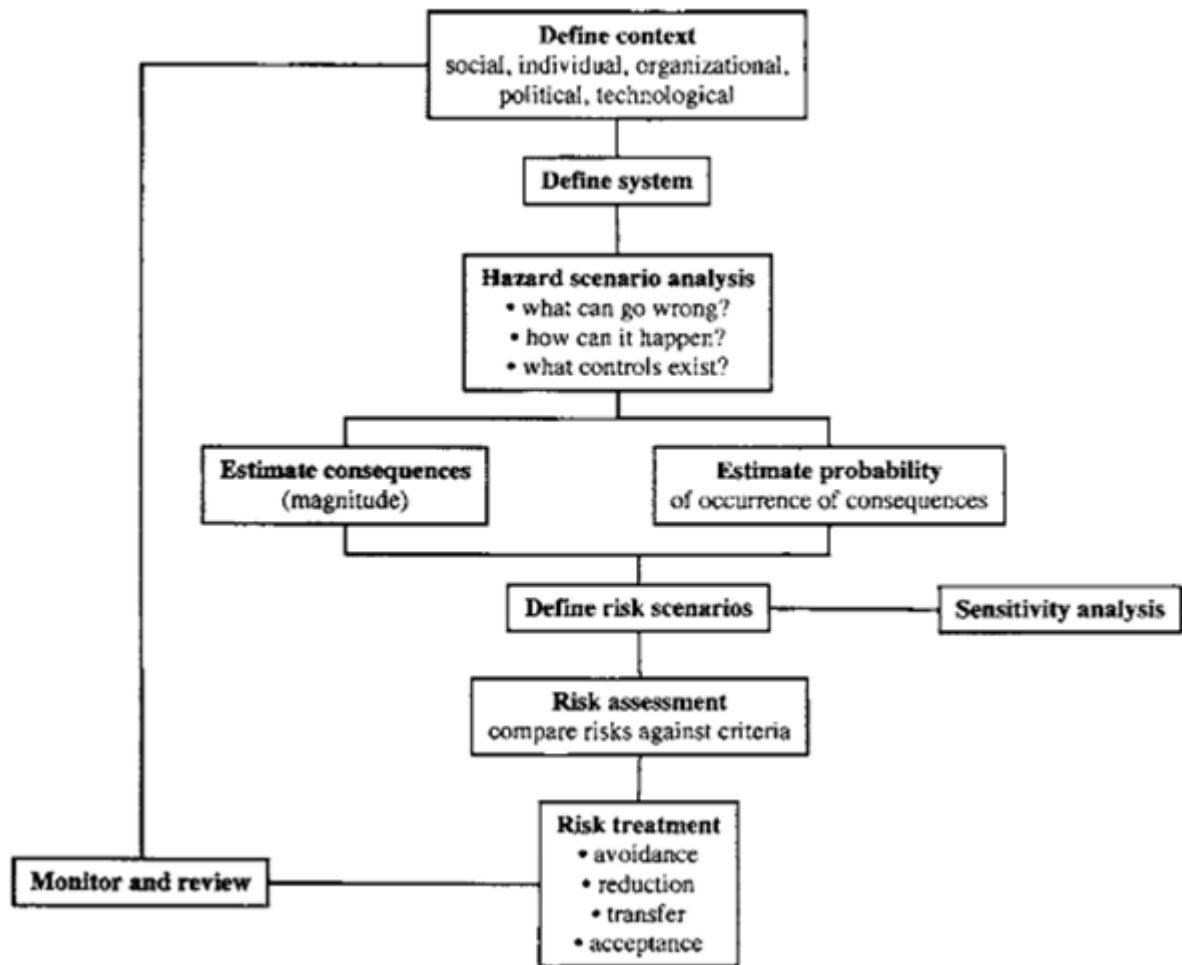


Figure 3.5 Generic Representation of Flowchart of risk based decision analysis

Most research and consulting activity related to blast damage has been limited to consequence analysis, namely, the system response (and associated damage and fatalities) given the detonation or release of a given amount of blast energy placed at some distance from a structure. Consequence analyses provide some information pertinent to assessing system vulnerability if the explosive weight, stand-off distance, and other loading and response parameters are known precisely. The level of risk or safety cannot be determined from such a deterministic analysis. The most recent reliability-based design and assessment techniques recognize that loads and capacities are variable in time and space and that these uncertainties need to be incorporated into any measure of safety used for decision making. Thus, modern-day code provisions for the design of structures to resist earthquakes, cyclones, snow, floods, and other natural hazards have been developed from the theories of probability and reliability (e.g., Ellingwood et al.1980). A PRA based on sound system and probabilistic modelling is well suited to predicting the future performance and reliability of blast damage to built infrastructure. Hence, a PRA is a useful mechanism to provide complementary information on the effectiveness of risk treatment options. A PRA may also be used:

1. By emergency services to predict the extent and likelihood of damage and casualty levels in contingency planning and emergency response simulations;
2. In collateral damage estimation for military planners _i.e., to minimize the risk of collateral damage when selecting size and delivery mode for military ordnance_; and
3. For security service forensics to back-calculate charge weights based on the known extent of observed damage and stand-off distance.

A PRA approach to decision making for blast damage to built infrastructure requires:

1. Predictive models for blast loads and system response;
2. Variability of input parameters and accuracy of predictive models;
3. Threat scenarios and their likelihood; and
4. Probabilistic and system reliability computations.

3.4. Uncertainty and Variability

There will be considerable uncertainty in blast loading and system response even if the explosive weight and stand-off distance are known precisely. This is because loading and system response models are subject to the following sources of uncertainty and variability:

1. Inherent variability: irreducible variability of the phenomenon itself;
2. Parameter uncertainty: uncertainty of input parameters used in predictive models; and
3. Model error: uncertainty in the accuracy of predictive models.

These three sources of uncertainty may also be categorized as

- aleatory (inherent variability)
- epistemic (parameter uncertainty)
- model error uncertainties.

These sources of uncertainty can be represented by probabilistic models. The inherent variability of system response is negligible if all parameters, predictive models, and threat scenarios are known precisely, because performance of man-made materials can, in principle, be estimated reasonably accurately. There will be inherent variabilities associated with blast pressure propagation that are likely to be high for complex blast environments.

Model error is defined as the actual loading/response divided by the model-predicted (theoretical)loading/response, with appropriate correction for experimental or measurement error

(e.g., Ellingwood et al. 1980). The model errors for system response generally are known only for failure modes (limit states) subject to static loading. This is not the case, however, for dynamic and impulse loading. Although a number of predictive models for blast loading and system response exist, much work remains to be done to fully validate many models with appropriate field and experimental data. This is not unexpected, because field and scale model tests are costly, and the tests themselves may introduce additional uncertainties during data interpretation and model validation. In the short term at least, the utility of risk assessment may be limited until robust predictive models can be validated and model errors quantified.

The variability and uncertainty of many system response parameters such as material properties and dimensions have been the subject of many studies. Probabilistic models for other parameters known to influence blast loading system response can be inferred from knowledge of physical limits on parameters and engineering judgment. Modelling the likelihood of explosive weight and stand-off distance is much more inexact, as this will be influenced by threat assessment. Nonetheless, scenarios can be hypothesized; for example, typical threat scenarios for a ground level detonation may include:

1. Explosive weight:

- 5kg (body explosive);
- 25kg (suitcase explosive); and
- 200 kg (car explosive), and so on.

2. Stand-off distance (protective barrier)

- 5 m from building; and
- 10 m from building, and so on.

For a particular threat scenario, assumptions can be made about likely TNT equivalence, type of explosive, etc. Calculated risks will be conditional on the incidence of a particular scenario. It is possible to aggregate these conditional risks if the probability of occurrence of each threat scenario (threat probability) is known or they can be hypothesized/inferred by expert opinion.

3.5. Reliability of Load Resisting Systems

Buildings, bridges, communication towers, dams, embankments, and other built infrastructure components represent “load resistance” or “demand-capacity” systems. These are substantial and expensive systems that tend to be unique or comprise “one off” elements. As such, their reliabilities cannot be directly inferred from observation of failures or other experimental studies. In these circumstances, reliabilities need to be calculated from predictive models and probabilistic methods. The probability of failure can be generalized as

$$P_f = \Pr[G(\mathbf{X}) \leq 0] \quad (3.11)$$

where $G(\mathbf{X})$ =limit state function; and \mathbf{X} =vector of all relevant variables.

Note that $G(\mathbf{X}) = 0$ defines the boundary between the “unsafe” and “safe” domains.

Usually, predictive models of system loading and response are incorporated into the limit state function(s). This general formulation can include system and time-dependent effects (e.g., Stewart and Melchers 1997; Melchers 1999).

A reliability analysis of blast damage to built infrastructure can be represented, for convenience, as having three levels, each level progressively requiring more probabilistic information and thus resulting in more useful probabilistic measures of reliability and decision support (see Fig.).

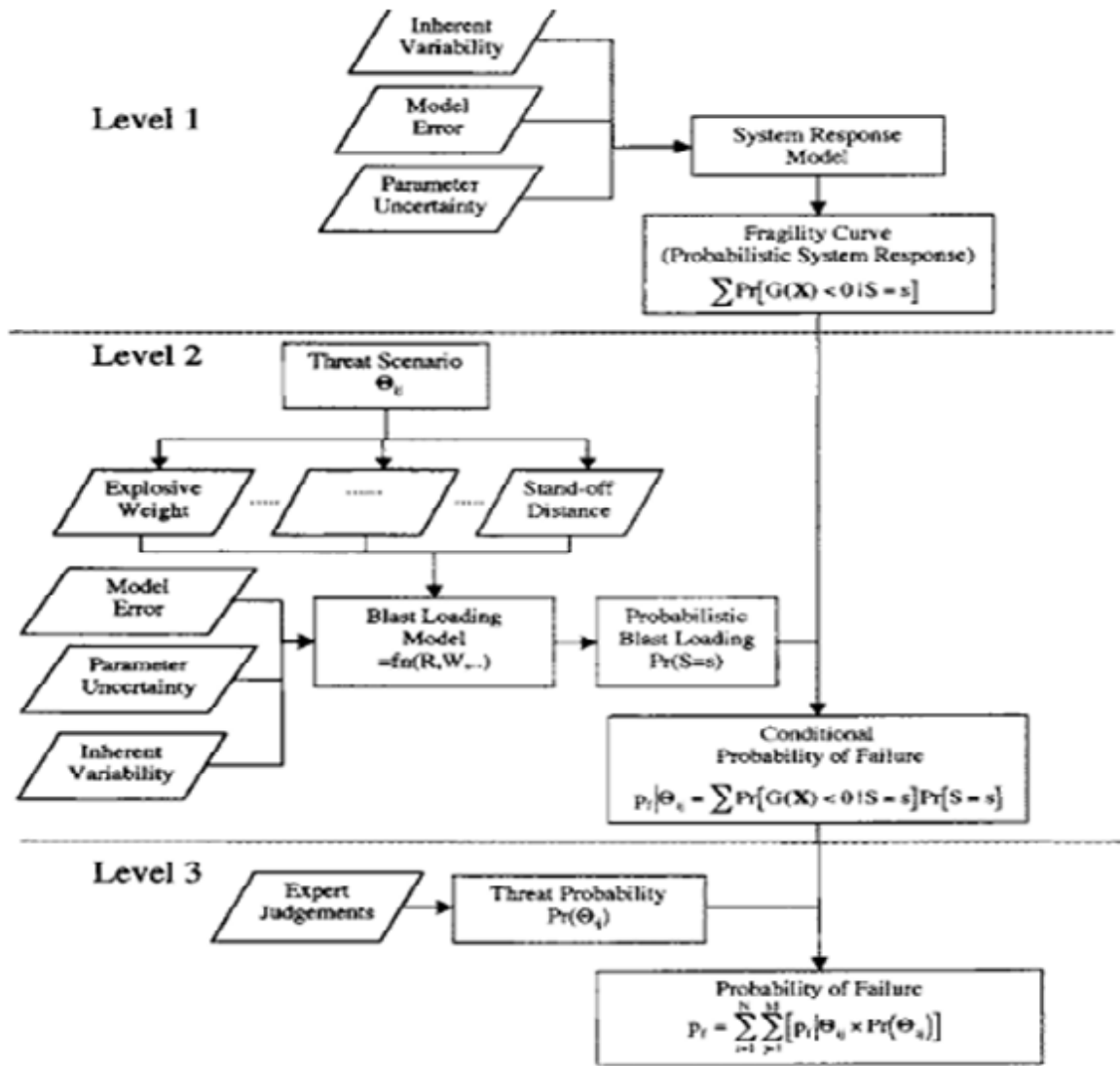


Figure 3.6 Illustrations of models and probabilistic data required for reliability analysis of blast damage to built infrastructure.

These are summarized as:

- Level 1: Fragility (or vulnerability) curves.
- Level 2: Probability of failure conditional on occurrence of a specific threat scenario. Blast reliability curves (BRC) can be generated from this information.
- Level 3: Probability of failure obtained from aggregation of conditional risks.

In the present case, the probability of failure conditional on the occurrence of a specific threat scenario is thus

$$P_f | \Theta_{ij} = \sum P_r [G(X) < 0 | S = s] P_r [S = s] \quad (3.12)$$

where

Θ_{ij} =threat scenario for a specific explosive weight i (e.g., $i =1$ for parcel bomb, $i =2$ for vehicle bomb, etc.)and stand-off distance j (e.g., $j =1$ for 5 m, $j =2$ for 10 m, etc)

$\Pr(S=s)$ represents the probability distribution of blast loading for a specific threat scenario (i.e., known explosive weight and stand-off distance) considering inherent model error and parameter uncertainties; and

$$\sum \Pr[G(X) < 0 | S = s] \quad (3.13)$$

represents the cumulative distribution function of resistance and is termed a fragility curve. A fragility curve is not dependent on load (hazard) modelling and so helps separate and identify the effect of resistance and load uncertainty on reliability calculations (e.g.Ellingwood and Tekie 2001; Rosowsky and Ellingwood 2002).

The epistemic and aleatory uncertainties can be propagated through the blast loading and system response computations to derive $\Pr(S=s)$ and fragility curves; see Fig. 3. The “failure region” denotes the region where there is a probability that loads (blast demand) will exceed resistance (capacity of the system to resist the blast demand).

A “blast reliability curve” (BRC) is a convenient way to summarize conditional probabilities of failure where one variable is fixed and the other given a range of values.

For example, a BRC can be a plot of probability of failure versus stand-off distance, for a specific explosive weight.

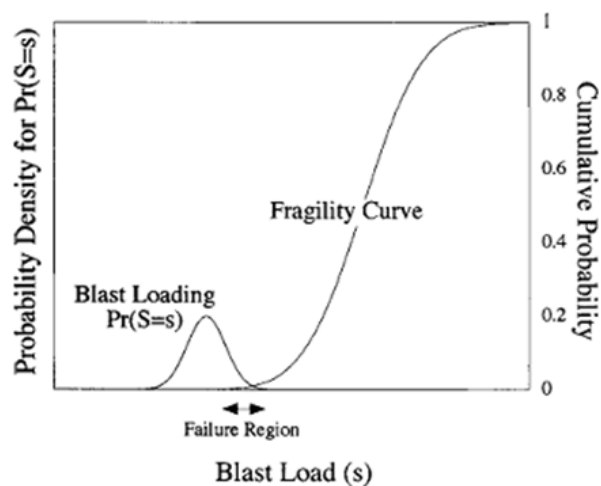


Figure 3.7 Illustration of variability of Blast loading and system response

Problem Definition

4.1. General

The steel framed structure which has been considered for blast loading is taken from “Energy flow in progressive collapse of steel framed building” by Stefan Szyniszewski .This is a typical low rise steel building in the USA. All prevailing requirements for gravity, wind, and seismic design have been considered. It was designed for a typical office occupancy live load of 2.5 kPa. The floors were assumed to support a dead load of 4 kPa, which included a concrete-steel composite slab, steel decking, ceilings/ flooring/fireproofing, mechanical/electrical/plumbing systems and partitions (1 kPa). The framing plan of the investigated 3-story building is shown in Fig. 9, Column schedules and beam designation are given in Table 2 and Table 3, respectively, with designations in accordance with AISC.

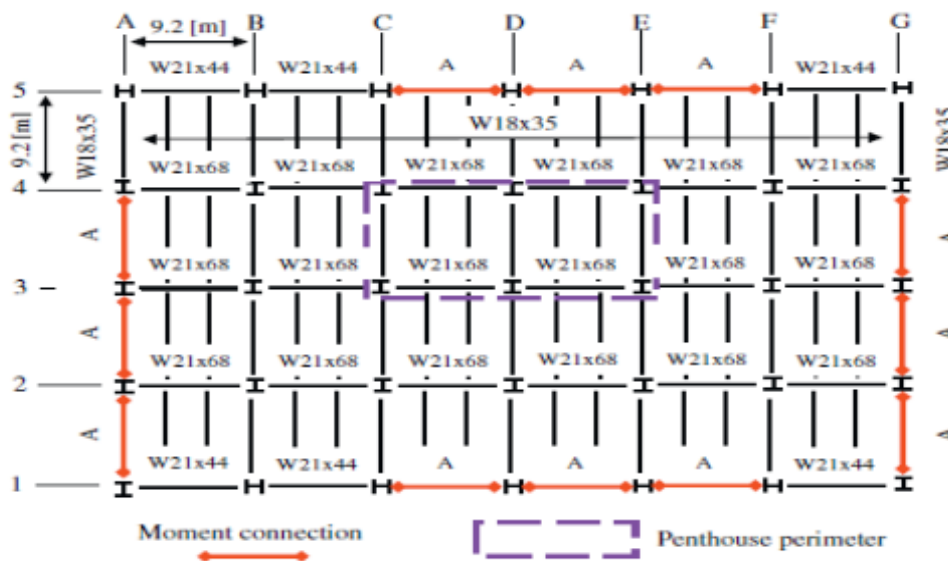


Figure 4.1 Framing Plan of the Steel Building, Courtesy “Energy Flow in Progressive Collapse of Steel Framed Building” By Stefan Szyniszewski

Table 4.1 Beams with Moment Resisting Connections Designated with “A”

FLOOR	2	3	ROOF
BEAM “A”	W18X35	W21X57	W21X62

Table 4.2 Steel Profiles of Columns

Floor No.	A	B	C	D	E	F	G
5	W12x58	W12x58	W14x74	W14x99	W14x99	W14x74	W12x58
4	W14x74	W12x58	W12x65	W12x72	W12x65	W12x58	W14x74
3	W14x99	W12x58	W12x65	W12x72	W12x65	W12x58	W14x99
2	W14x99	W12x58	W12x58	W12x58	W12x58	W12x58	W14x99
1	W14x74	W12x58	W14x74	W14x99	W14x99	W14x74	W14x74

4.2. Modelling of the Steel Building in SAP2000® and Assignment of Dead and Live Load

The following pictures represent the various stages of the designing of the building considered:

1. Modelling of the building’s first floor and assignment of joint fixities :

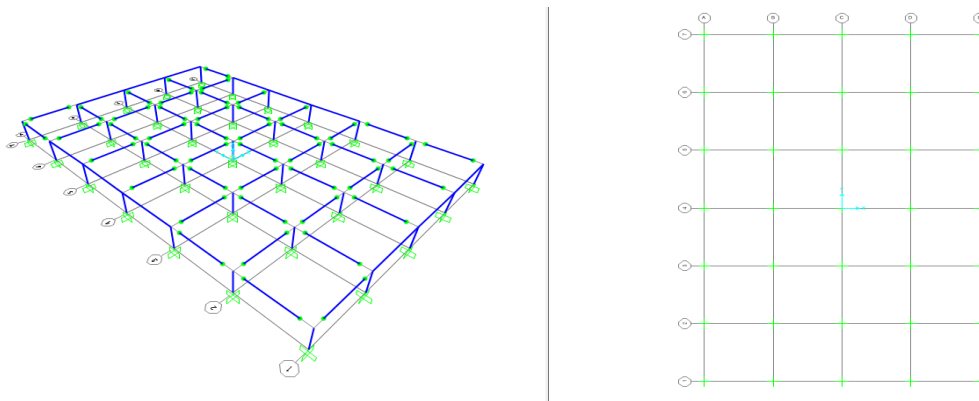


Figure 4.2 Building’s first floor- Model

2. Assignment of respective steel sections with corrected Orientation:

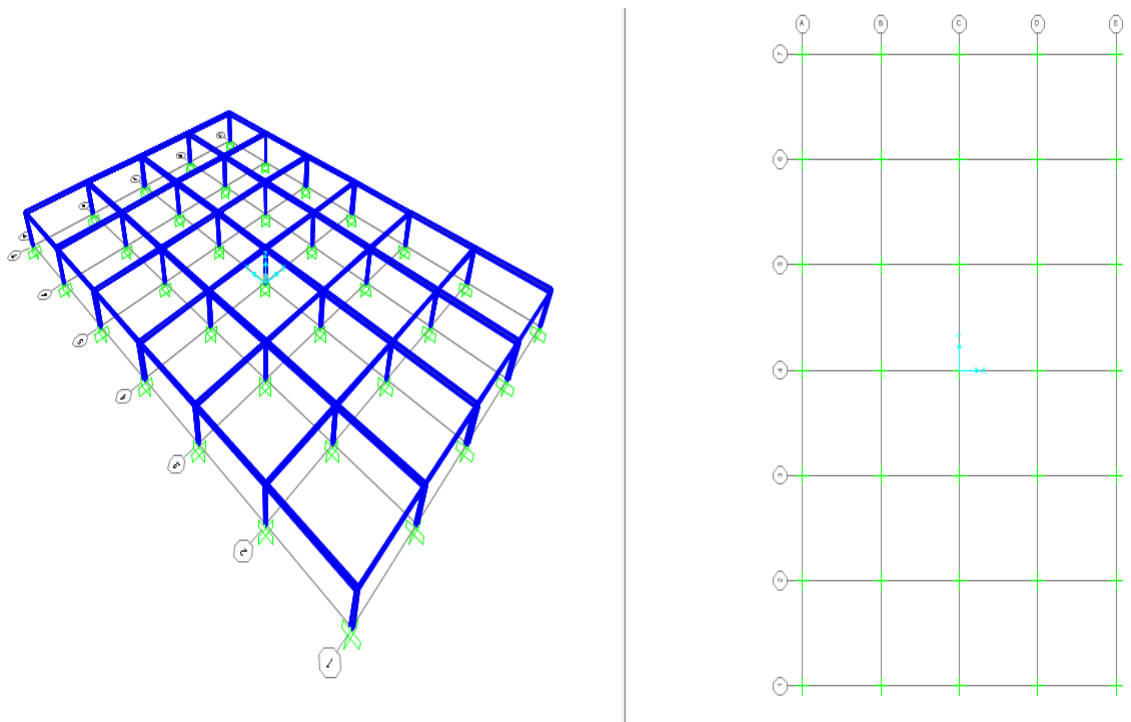


Figure 4.3 Building's first floor- With steel sections

3. Assignment of Floor properties and Dead and Live Loads:

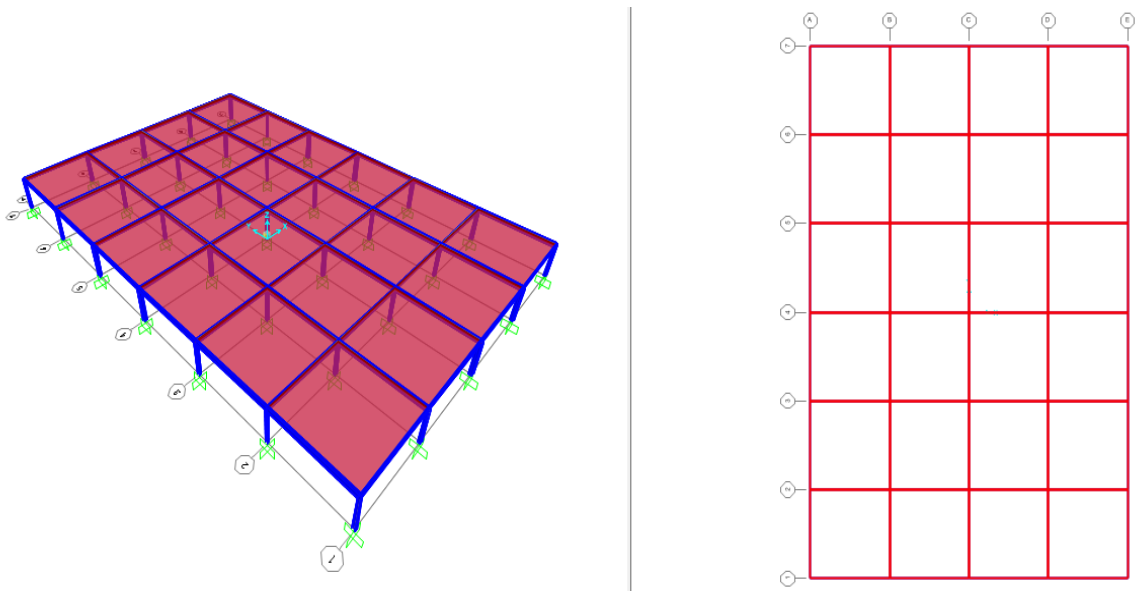


Figure 4.4 Building's first floor with slab

4. Replication of the Remaining two floors with correct beams on each floor:

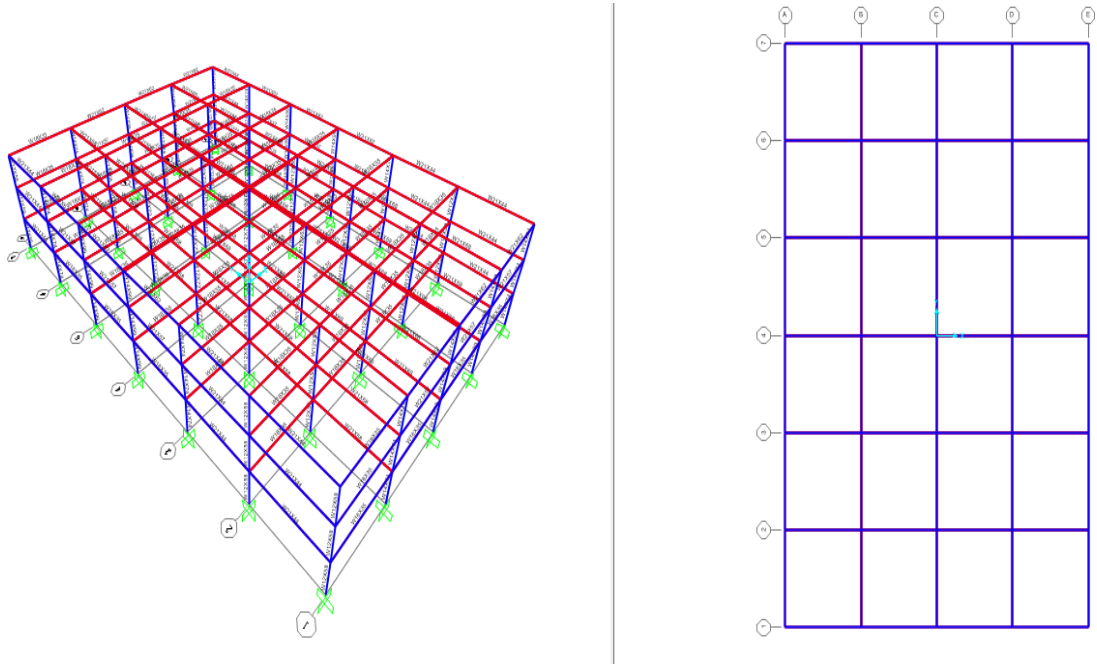


Figure 4.5 Three floors of building- Model

5. The complete building with loads applied on each floor:

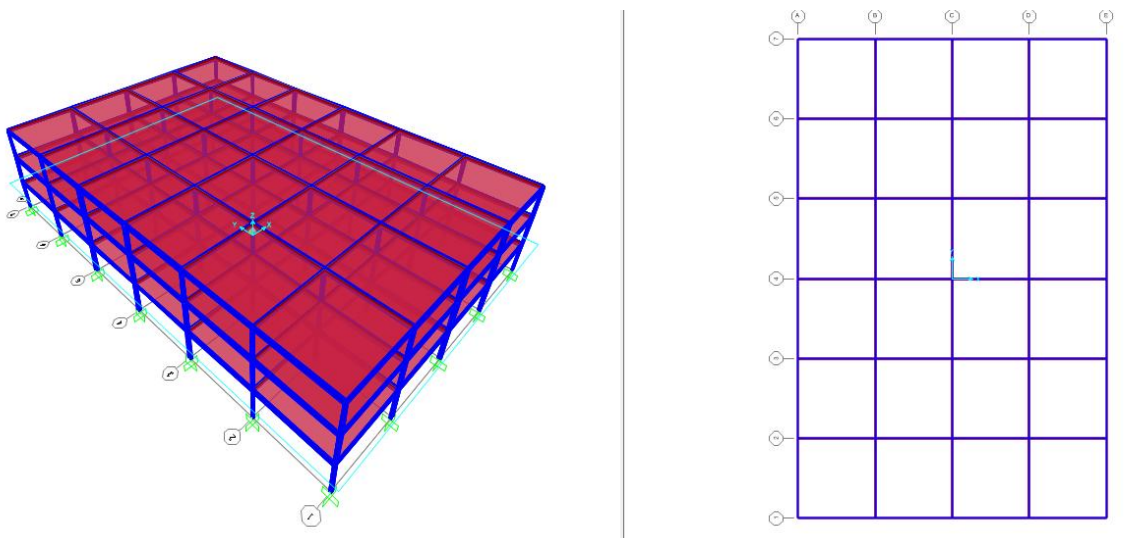


Figure 4.6 Three floors of building with slab

Blast Pressure Computations

5.1 Calculating the Peak Overpressure

A program has been developed in MS Excel to compute the Peak Incident Pressure, Positive Time duration, Positive Impulse and Peak Reflected Pressure, for various values of R and W using Kinney and Graham's approach.

The results of the program for R = 5m and W = 20 kg and angle of incidence = 0 degree is as follows:

Table 5.1 Blast Pressure Calculation

			<u>BLAST PRESSURE CALCULATION</u>		
Radial distance (R)	5	m			
Charge Wt (W)	20	kg			
Angle of Incidence	0	Degree			
Scaled Distance (Z)	1.843856	$m/kg^{1/3}$	1 bar =	14.50377	Psi
			Peak incident pressure (in psi)	35.97857	
Peak Incident Pressure	2.480635	bar			
Positive Time Duration	19.50525	msec	T	0.1	Sec
Posittive Impulse(<i>Ipos</i>)	0.911542	bar-ms			
Wave Decay Parameter (b)	0.777538				

Coefficient of Reflection at 0 degree	2.35				
Peak Ref Pressure(Pref)	5.829492	bar			

5.2 Calculation of the Peak Reflected Pressure

STEP 1: Calculation of the Angle of Incidence, α

The angle of incidence is defined as the angle made by the blast wave propagating towards the surface of the structure with its normal. UFC 3-340-02 gives the detailed procedure of determining the peak reflected pressure on a surface depending upon the peak incident pressure and angle of incidence of the waves.

In present approach, a program has been developed in MS excel to find the angle of incidence depending upon the coordinates of the points and standoff distance. The same is included in appendix -A of this report.

The following figure shows the diagrammatic representation of the program and its significance:

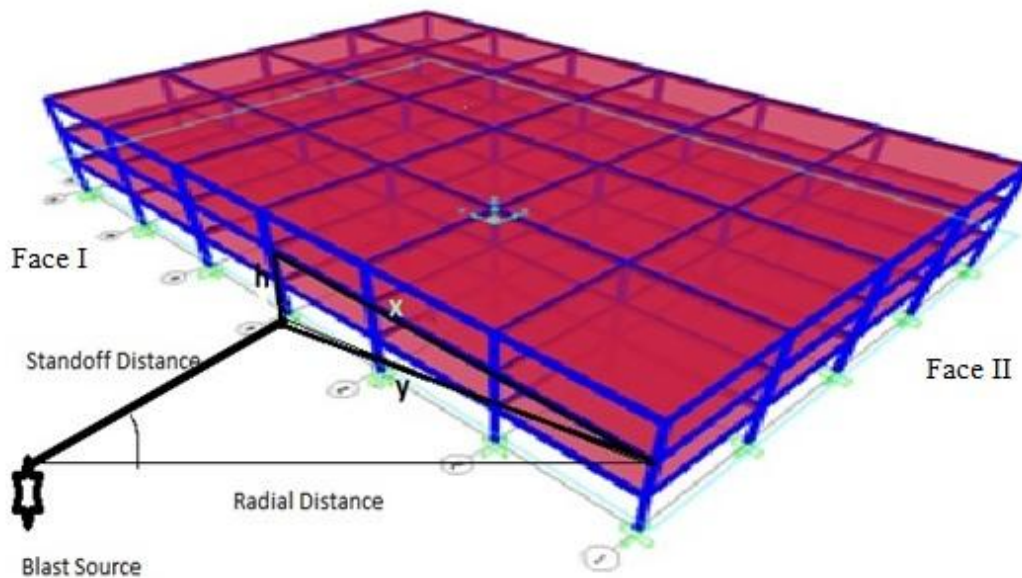


Figure 5.1 The scaled distance, standoff distance, x, y, h and angle of incidence

The program for the standoff distance 5m and the blast load on one face of the building has been included in appendix- B of this report.

STEP 2: Calculations of Peak Incident Overpressure, Positive Time Duration, Positive Impulse(Ipos), Wave Decay Parameter :

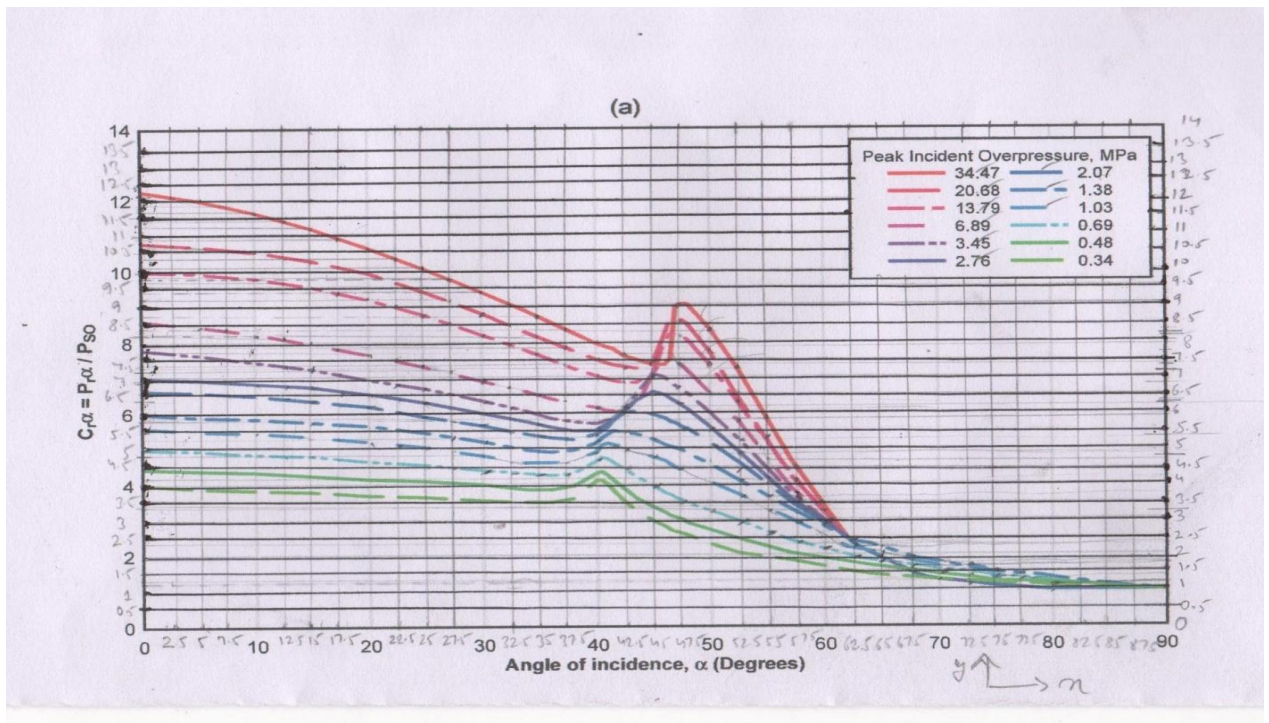
The calculated values of the radial distance and given value of charge weight are used to calculate the Peak Incident Overpressure, Positive Time Duration, Positive Impulse(Ipos), Wave Decay Parameter, using the Kinney Graham Approach.

A MS excel program has been developed for the same calculations and these have been included in appendix- B..

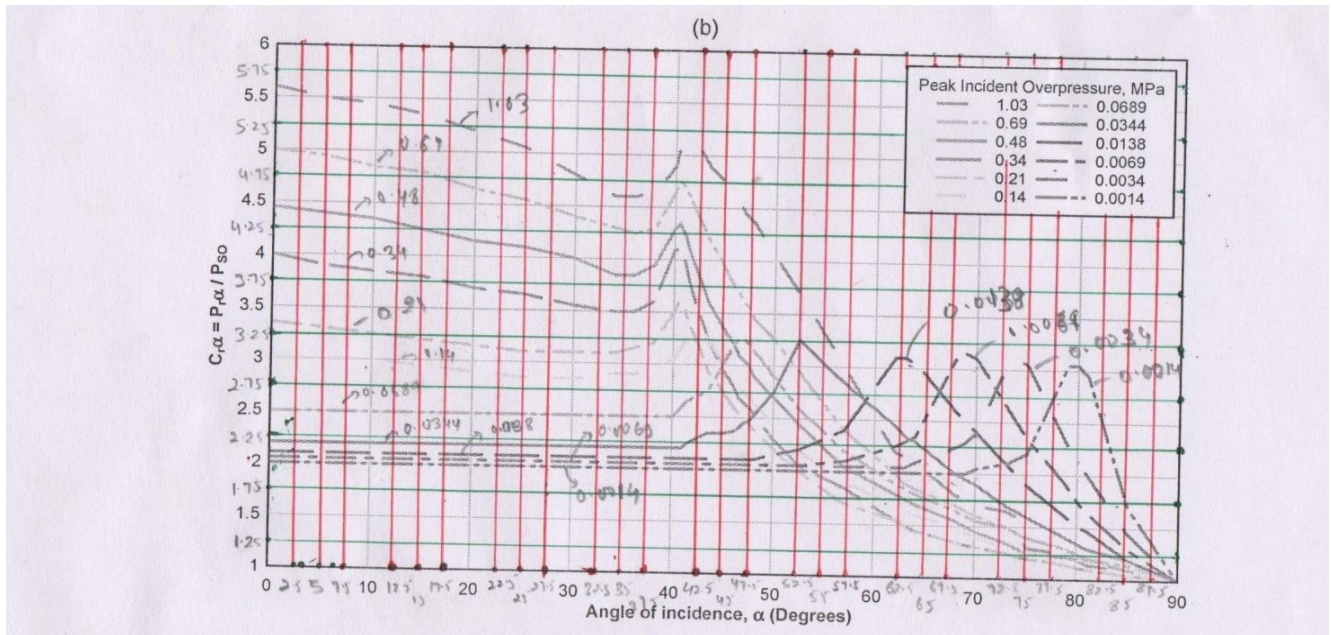
STEP 3: Calculations of the Coefficient of Reflection and Peak Reflected Overpressure:

The coefficient of reflection has been derived from the graphs given by Mays and Smith and UFC 3-340-02 (2008).

For the derivation of the coefficient of reflection the graphs given were discretized and the corresponding values were recorded in MS excel sheets. The following diagram shows the discretized graphs:



(a)



(b)

Figure 5.2 The UFC 3-340-02 (2008) graphs (discretized)

After the simplification of the above graphs the MS Excel sheets were obtained that contained the different values of coefficient of reflection for various values of the peak pressure and angle of incidence.

Following this process the Peak Reflected Overpressure has been calculated by using the values of the coefficient of reflection obtained.

5.3 Computation of the peak pressures at the different joint of the structure resulting from an explosion

1. To find out the incident pressure duration, Kinney and Graham's (1985) empirical relations reported in Goel et al. (2012) are used. The positive phase durations (t_{pos}) are based on the scaled distance (Z) in $m/kg^{1/3}$
2. The reflected positive phase duration is taken equal to the duration of the incident positive pressure phase, as the difference is very small. The negative phase of the pressure time history is neglected in the present approach.
3. The distributions of the blast pressure from the walls to the joints are taken as given in the Figure. The structures are analyzed by considering only the peak pressure are acting on the joints and the detonation points to be in front of different faces of the buildings based on column orientations (I-section).

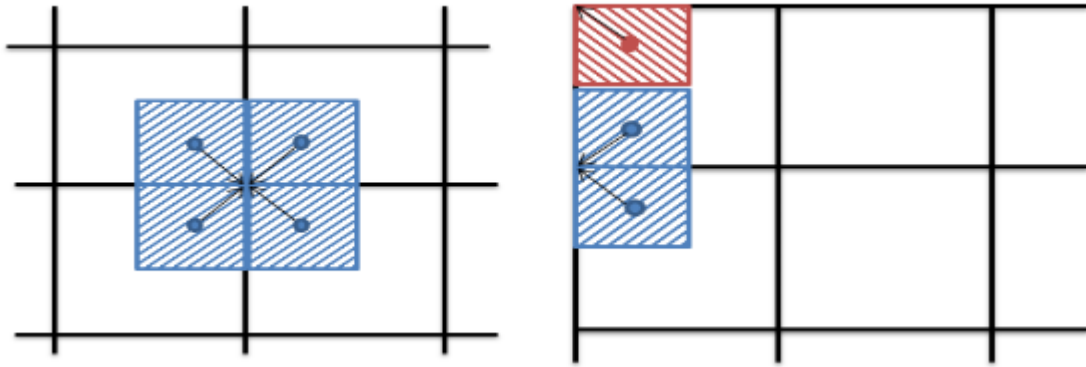


Figure 5.3 Distribution of Blast Pressure From Walls To Joints.

In case of the building taken in this report the following calculations have been used to find the blast load at various joints and walls of one face of the building.

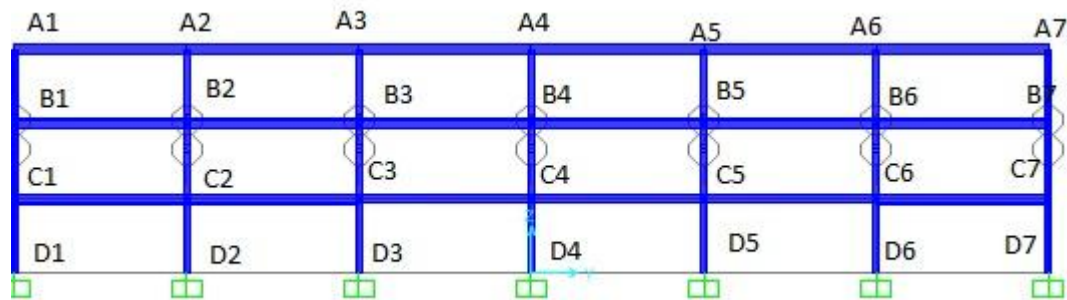


Figure 5.4 The face of building considered for computations.

The load due to blast on the walls and the joints of the building are computed using the:

- i. Peak reflected overpressure obtained from the Excel program
- ii. The area over which the blast pressure is distributed.

Such that,

- a. P_{ref} on joint A1 = 18 kN/m² (as calculated from sheet)

$$\text{Area of the pressure on joint A1} = \frac{9.15}{2} \times \frac{3.96}{2} = 9.0585 \text{ m}^2$$

$$\text{The load on joint A1} = PA1 = 18 \times 9.0585 = 163.053 \text{ kN}$$

- b. P_{ref} on joint A2 = 31 kN/m²

$$\text{Area of the pressure on joint A2} = 9.15 \times 3.96 / 2 = 18.117 \text{ m}^2$$

$$\text{The load on joint A2} = PA2 = 31 \times 18.117 = 561.627 \text{ kN}$$

- c. P_{ref} on joint B2 = 36 kN/m²

Area of the pressure on joint B2 = $9.15 \times 3.96 = 36.234 \text{ m}^2$

The load on joint B2 = $PB2 = 36 \times 36.234 = 1304.424 \text{ kN}$

Similarly, the following are the calculated values of the load, due to blast on the joints and the corresponding values of the positive phase durations (t_{pos}), as obtained from the sheets.

Table 5.2 The Computed Blast Load On Each Joint Of The Face

JOINT	BLAST LOAD(kN)	t_{pos} (milliseconds)
A1/106	163.053	158
A2/107	561.627	103.43
A3/108	1123.245	66.78
A4/109	1739.232	52.61
A5/110	1123.25	66.78
A6/111	561.627	103.43
A7/112	163.053	158
B1/71	362.34	148.24
B2/72	1304.424	92.55
B3/73	3369.762	53.54
B4/74	7246.8	36.88
B5/75	3369.762	53.54
B6/76	1304.424	92.55
B7/77	362.34	92.55
C1/2	380.457	142.23
C2/4	1485.594	85.81
C3/6	4855.356	44.68
C4/8	17682.192	24.05
C5/10	4855.356	44.68
C6/12	1485.594	85.81
C7/14	380.457	142.23
D1/1	190.22	140.20
D2/3	760.914	83.52
D3/5	2826.252	41.49
D4/7	15290.748	17.36
D5/9	2826.252	41.49

D6/11	760.914	83.52
D7/13	190.22	140.20

5.4 Variation of Peak Reflected Pressure as per Kinney and Graham

Graphs showing the plot of the Peak Reflected Pressure (P_{ref}) in kN/m^2 vs. Radial Distance (R) in m have been plotted for different values of the charge weight (W) in kg.

The following are the plots for different values of the angle of incidence.

1. Angle of incidence = 0° :

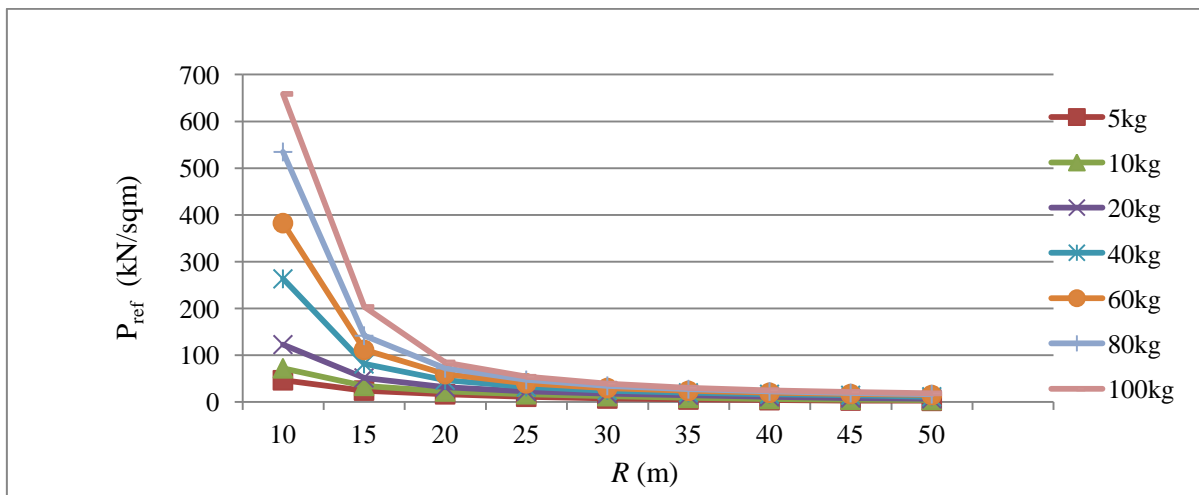


Figure 5.5 Plot between P_{ref} vs. R for $\alpha = 0^\circ$

2. Angle of incidence = 15°:

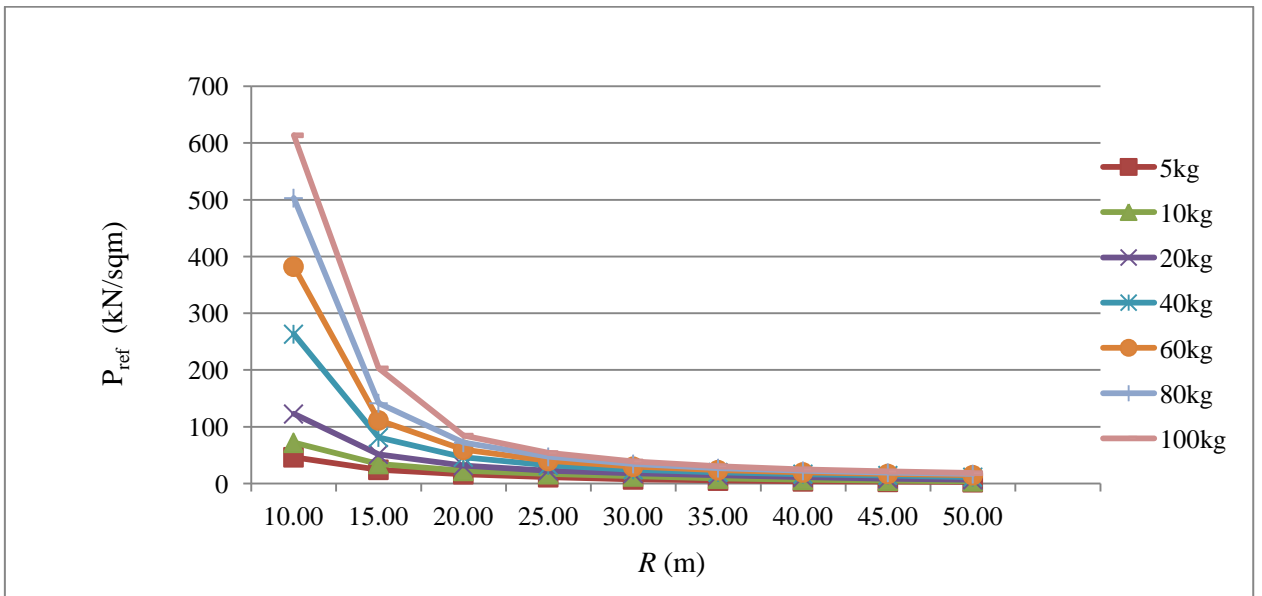


Figure 5.6 Plot between P_{ref} vs. R for $\alpha = 15^\circ$

3. Angle of incidence = 20°:

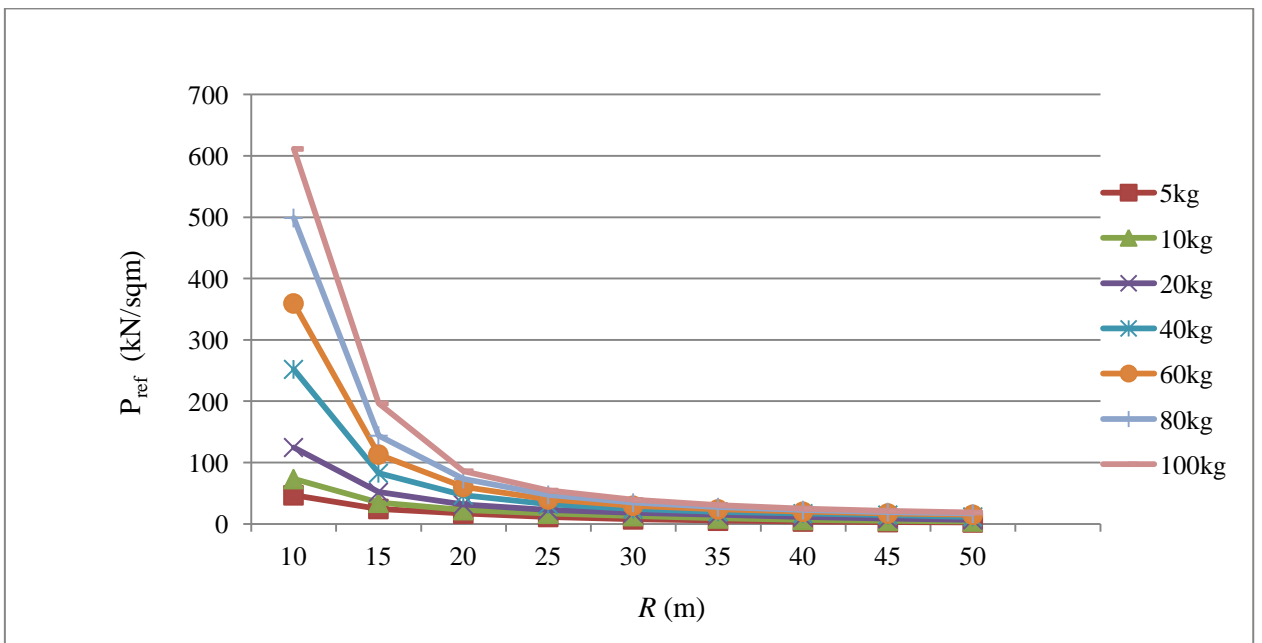


Figure 5.7 Plot between P_{ref} vs. R for $\alpha = 20^\circ$

4. Angle of incidence = 30°:

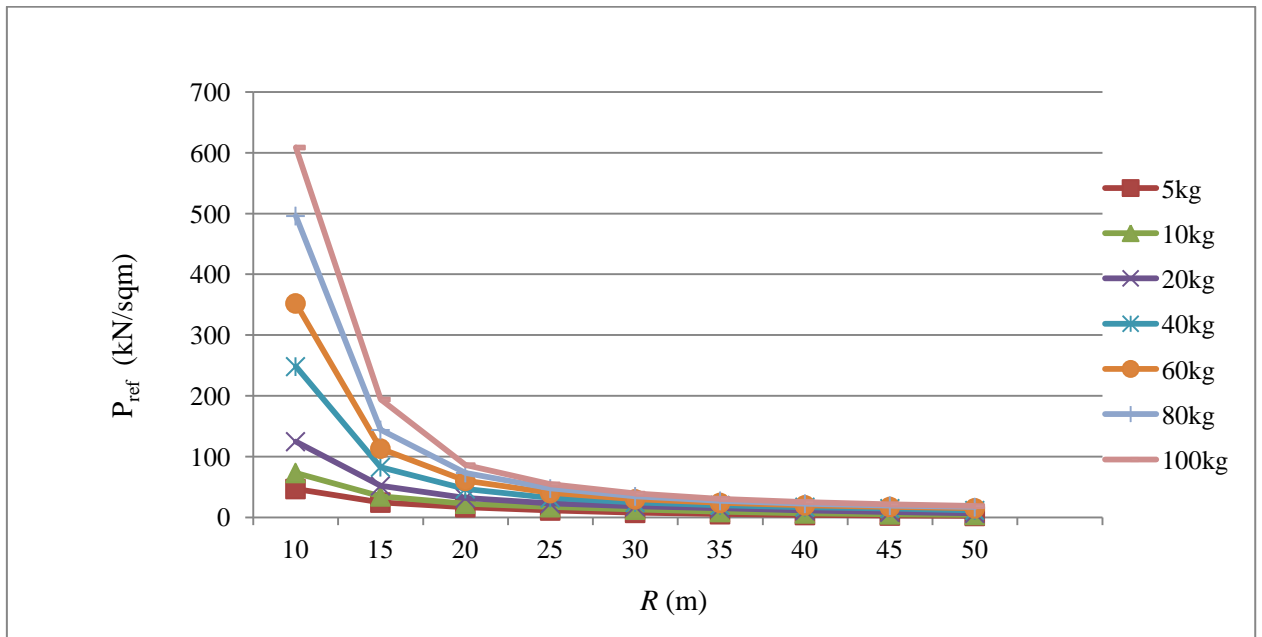


Figure 5.8 Plot between P_{ref} vs. R for $\alpha = 30^\circ$

5. Angle of incidence = 45°:

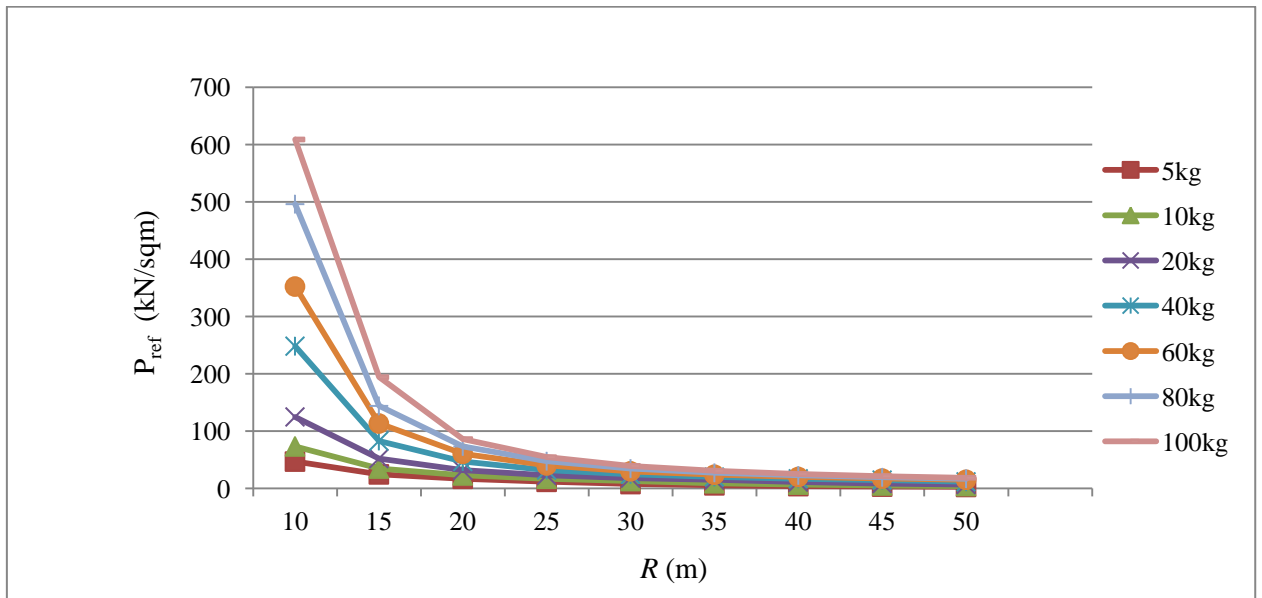


Figure 5.9 Plot between P_{ref} vs. R for $\alpha = 45^\circ$

6. Angle of incidence = 60° :

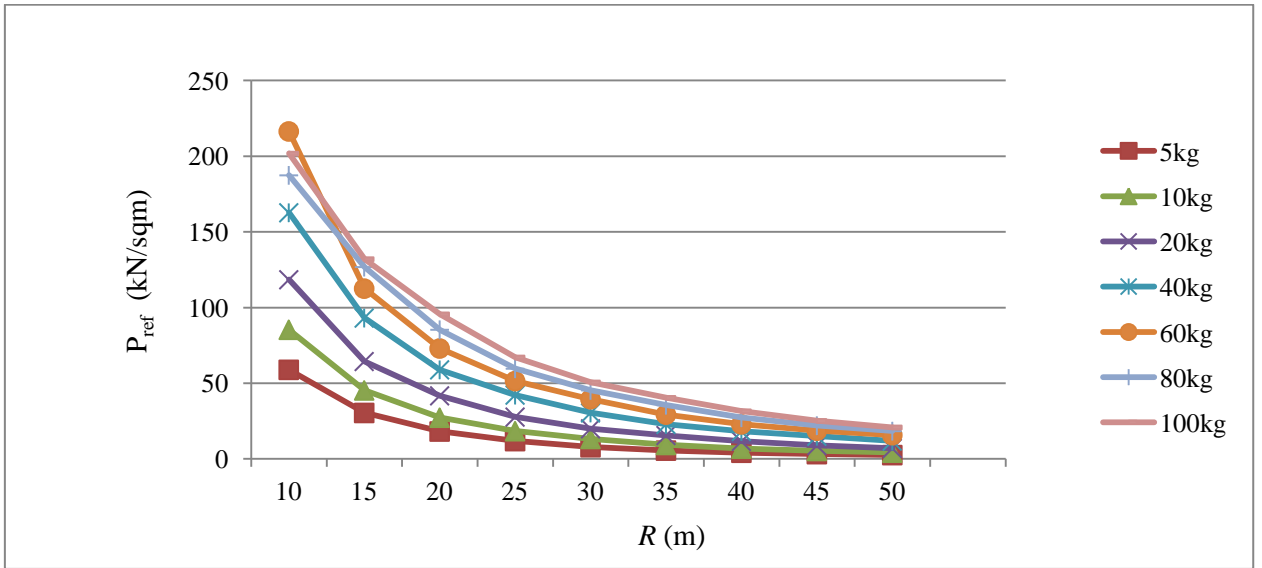


Figure 5.10 Plot between P_{ref} vs. R for $\alpha = 60^\circ$

7. Angle of incidence = 75° :

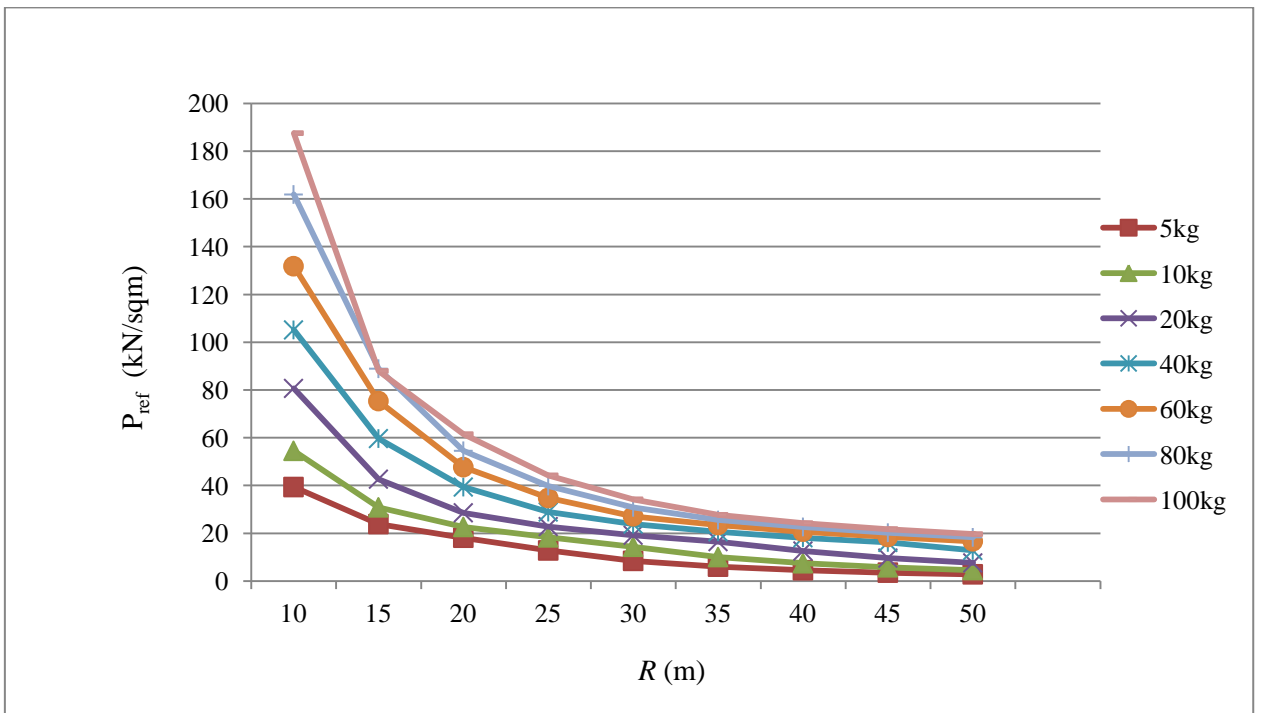


Figure 5.11 Plot between P_{ref} vs. R for $\alpha = 75^\circ$

8. Angle of incidence = 90°:

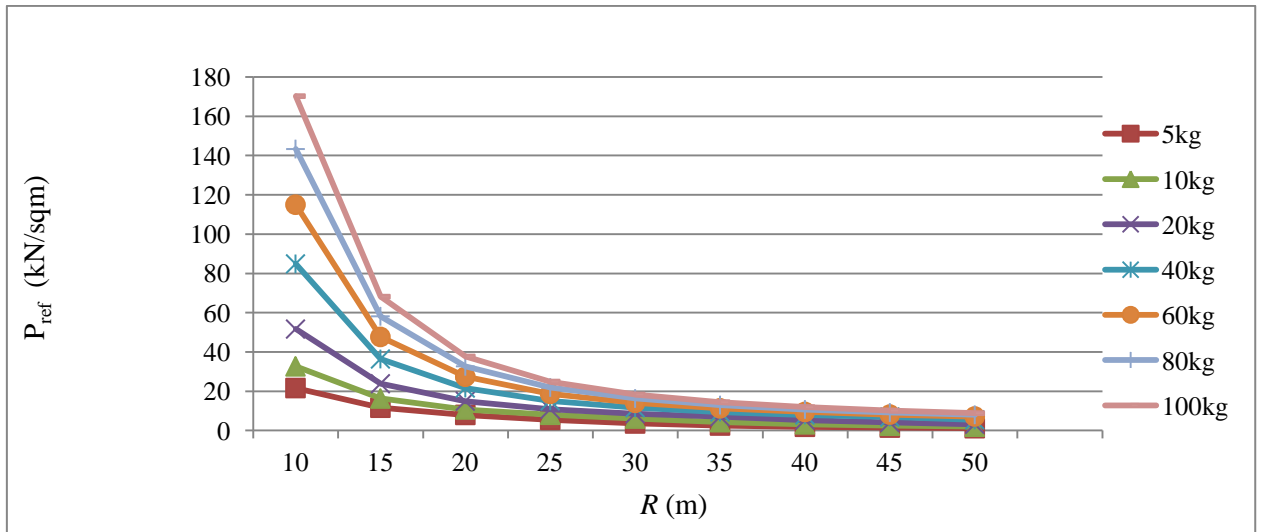


Figure 5.12 Plot between P_{ref} vs. R for $\alpha = 90^\circ$

5.5 Observations from the Plots

After analysing the plots for different values of angle of incidence the following observations are evident:

1. The value of peak reflected pressure as evident from the plots is very high for the radial distance up to 10 m and there is a significant drop in the values of the peak reflected pressure from 10 m to 20 m.
2. Also, the values of the peak reflected pressure, for all charge weights, is low for all the radial distances beyond 20 m.
3. This implies that the parking lots should not be constructed in front of the face of the building and a minimum distance from the face of the building should be 10 m.
4. The parking lots should always be constructed at the corners, such that the angle of incidence of the blast load to the main structural frame of the building always produces high values. Keeping the angle of incidence values high causes the blast load to be reduced significantly.

5. The parking lots should never be constructed near the entrant corners of the building as the radial distance to the entrant corner of the building will be less than 10 m and the values of the angle of incidence will be high for the same scenario.

Statistical Properties of Charge Weight and Output Quantities

6.1. Statistical Properties Studied

The following terms of probability theory need to be considered before progressing towards the assessment of the charge weights and bending moments.

1. Normal Distribution

In probability theory, the normal (or Gaussian) distribution is a very common continuous probability distribution. In its most general form, under some conditions (which include finite variance), it states that averages of random variables independently drawn from independent distributions converge in distribution to the normal, that is, become normally distributed when the number of random variables is sufficiently large. The normal distribution is sometimes informally called the bell curve.

2. Arithmetic Mean

In mathematics and statistics, the arithmetic mean or simply the mean or average is the sum of a collection of numbers divided by the number of numbers in the collection. The collection is often a set of results of an experiment, or a set of results from a survey.

3. Standard Deviation

The standard deviation (SD, also represented by the Greek letter sigma σ or s) is a measure that is used to quantify the amount of variation or dispersion of a set of data values. A low standard deviation indicates that the data points tend to be close to the mean (also called the expected value) of the set, while a high standard deviation indicates that the data points are spread out over a wider range of values.

4. Skewness

Skewness is a measure of the asymmetry of the probability distribution of a real-valued random variable about its mean. The skewness value can be positive or negative, or even undefined.

5. Kurtosis

Kurtosis (meaning "curved, arching") is a measure of the "tailedness" of the probability distribution of areal-valued random variable. In a similar way to the concept of skewness, *kurtosis* is a descriptor of the shape of a probability distribution.

6. Coefficient of Variation

The coefficient of variation (CV), also known as relative standard deviation (RSD), is a standardized measure of dispersion of a probability distribution or frequency distribution. It is often expressed as a percentage, and is defined as the ratio of the standard deviation σ to the mean μ (or its absolute value, $|\mu|$).

6.2. Face I of the Building

The following are the different plots and values for the face I of the building:

1. Plot between the **Probability Density Function (PDF) and the Charge Weight**:

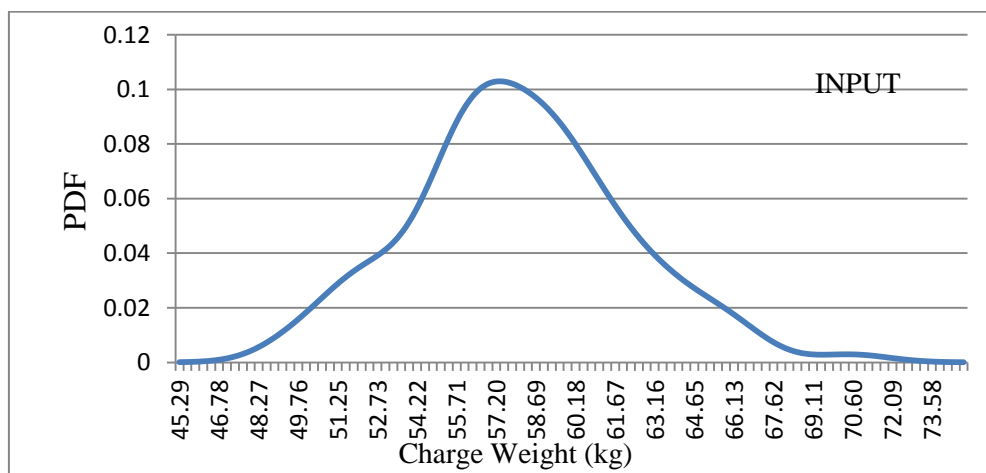


Figure 6.1 Plots for Charge Weight

- a. Arithmetic mean – 60.03 kg
- b. Standard Deviation – 8.63
- c. Skewness – 0.2717
- d. Kurtosis – 3.188
- e. Coefficient of Variation- $(8.63/60.03) = 0.144$

2. Plot between the **Probability Density Function (PDF) and Bending Moment:**

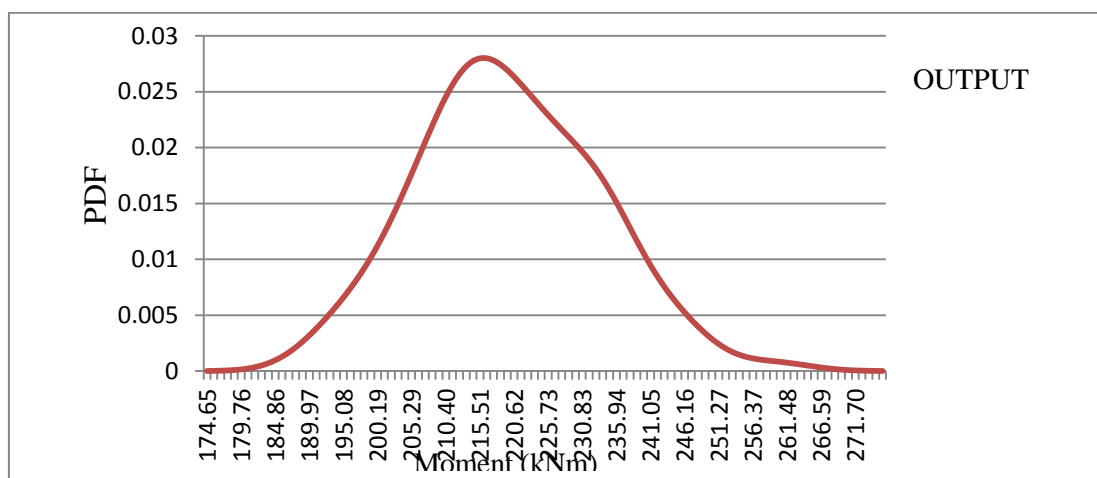


Figure 6.2 Plots for Bending Moment

- a. Arithmetic mean – 225.21 kNm
- b. Standard Deviation – 29.63
- c. Skewness – 0.2453
- d. Kurtosis – 2.8769
- e. Coefficient of Variation- $(29.63/225.21) = 0.131$

6.3. Face II of the Building

The following are the different plots and values for the face II of the building:

1. Plot between the **Probability Density Function (PDF)** and the **Charge Weight**:

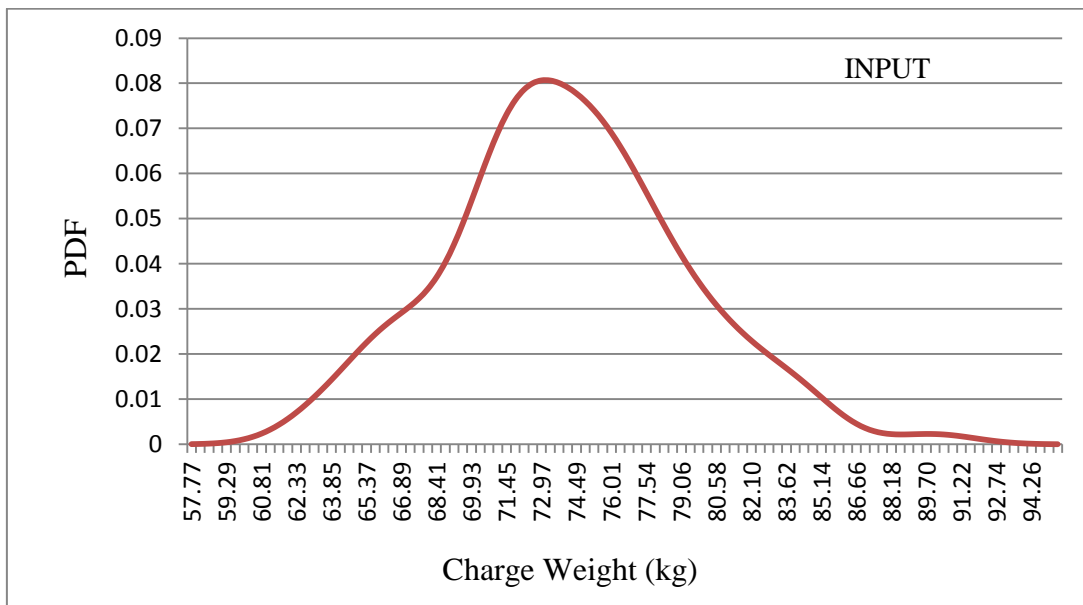


Figure 6.3 Plots for Charge Weight

- a. Arithmetic mean – 76.58 kg
- b. Standard Deviation – 11.028
- c. Skewness – 0.2707
- d. Kurtosis – 3.1869
- e. Coefficient of Variation- $(11.028/76.58) = 0.144$

2. Plot between the **Probability Density Function (PDF) and Bending Moment:**

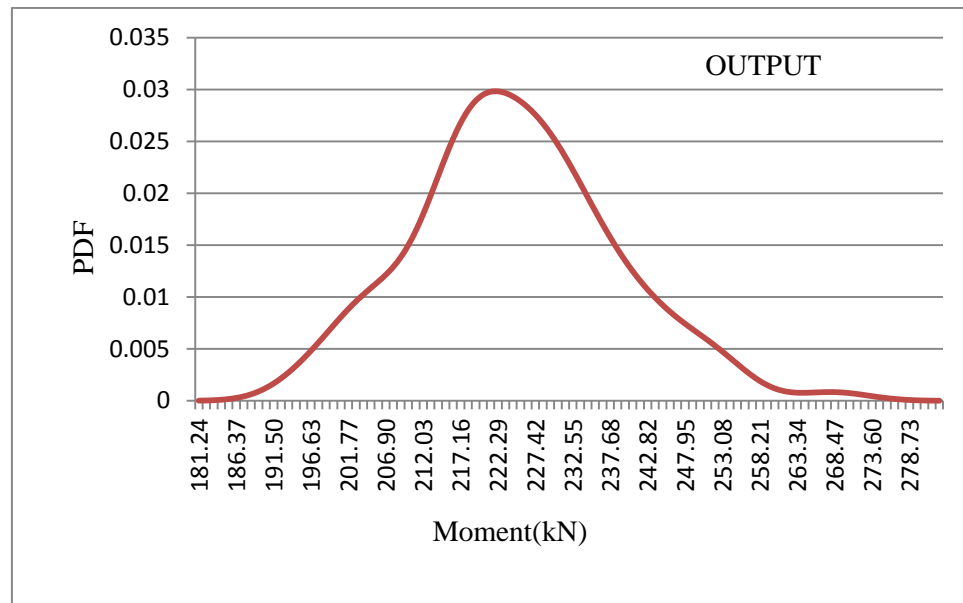


Figure 6.4 Plots for Bending Moment

- a. Arithmetic mean – 232.04 kNm
- b. Standard Deviation – 29.77
- c. Skewness – 0.3266
- d. Kurtosis – 3.2259
- e. Coefficient of Variation- $(29.77/232.04) = 0.128$

6.4. Discussion of the Results

1. For the face I of the building the coefficient of variation for charge weight is 0.144 while that for the moment is 0.131. This implies that the effect of uncertainty in the values of the charge weight does not magnify the effect of uncertainty in the values of bending moments.
2. Similarly, for the face II of the building the coefficient of variation for charge weight is 0.144 while that for moment is 0.128. This implies that the effect of uncertainty in the values of the charge weight does not magnify the effect of uncertainty in the values of bending moments.
3. Since the values of the skewness and kurtosis is near in both the cases so there is no significant variation in terms of skewness and kurtosis.

Time-History Analysis of the Structure

7.1. Assigning of the Time-History Loads

Time-history analysis provides for linear or nonlinear evaluation of dynamic structural response under loading which may vary according to the specified time function.

The loads computed above along with their respective positive phase durations (t_{pos}) have been used to time history loading on the different joints of the structure.

The following diagram is an example of the triangular load on the structures:

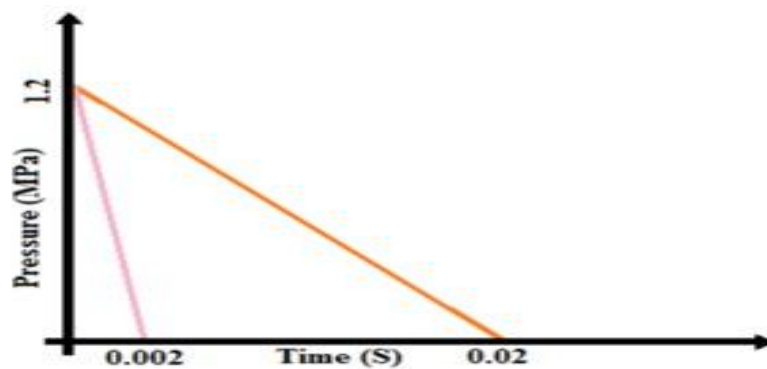


Figure 7.1 An example of the triangular load.

The following procedure has been adopted to apply the time history load on one of the face of the structure:

1. The values of the load and their respective positive phase time have been used to define the time history load cases for different joints, by using Define>Function>Time History in SAP2000.
2. Each type of load pattern has been defined for different joints by using Define>Load pattern.
3. Different load cases have been defined for each load by using Define>Load cases and defining loads type as Time History for time history load.
4. The load combinations have been created
 - One for the DL+ LL+ Time History Loads

- One for only Time History Loads
5. The loads are assigned for each type of load combination on the respective joint.
 6. After the loads have been assigned the analysis is run.

7.2. Results of the Analysis

The following are the results after the analysis is run under different combinations:

1. Under Time History Loading only :

- a. The behaviour of full structure:

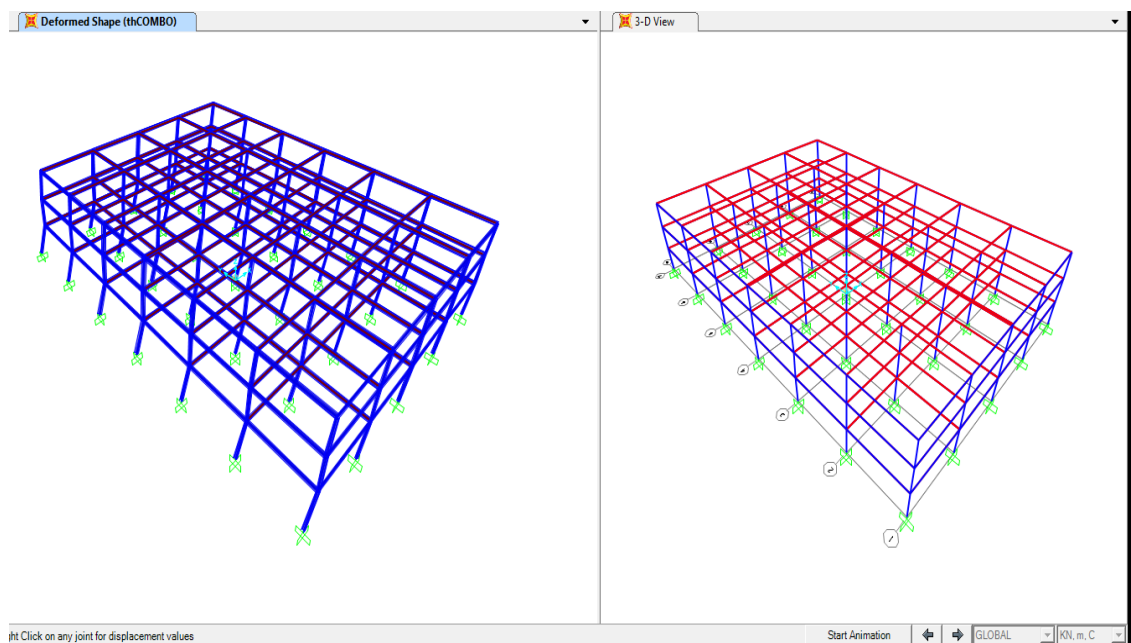


Figure 7.2 The behaviour of full structure, under Time History Loading only

b. The behaviour of the one of the faces:

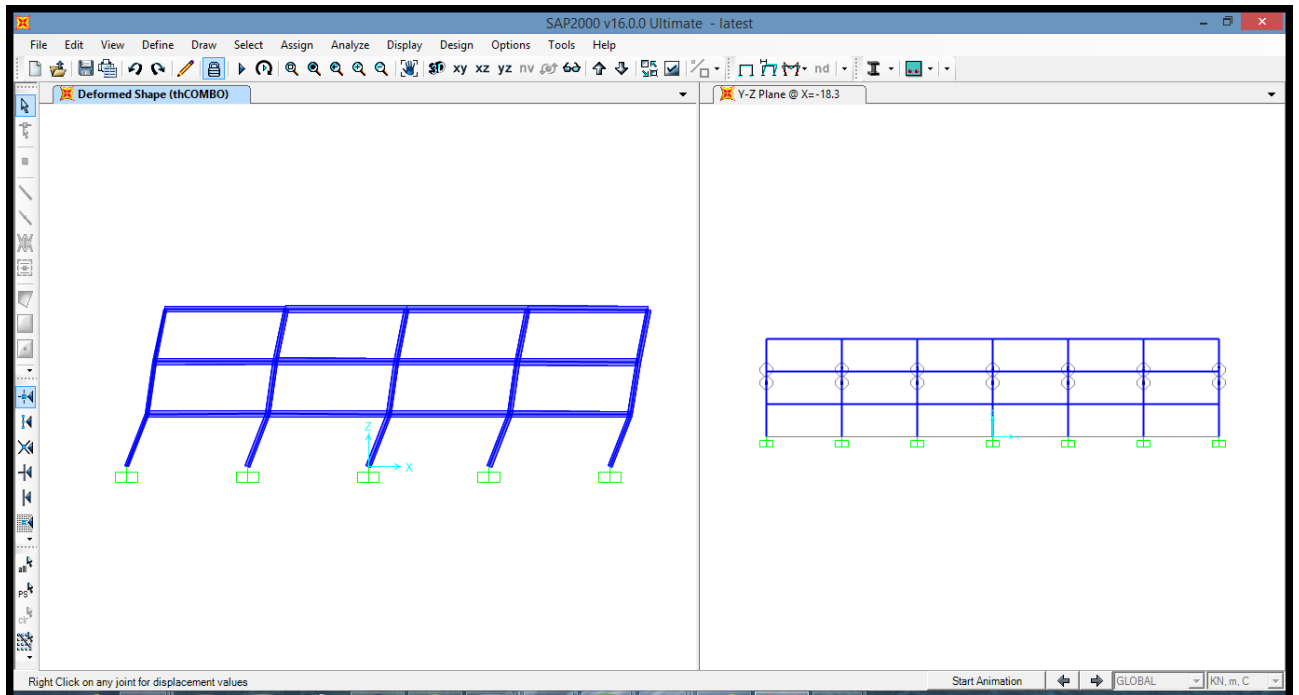


Figure 7.3 The behaviour of the one of the faces, under Time History Loading

c. The display plot function of joint A1:

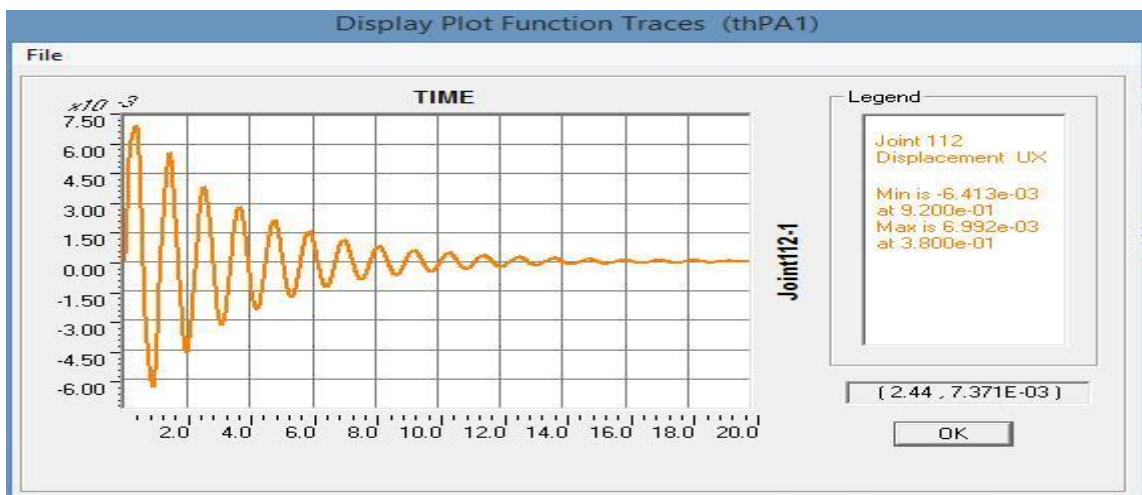


Figure 7.4 The display plot function of joint A1

2. Under the combination of the DL+LL+ Time History Loading:

a. The behaviour of full structure:

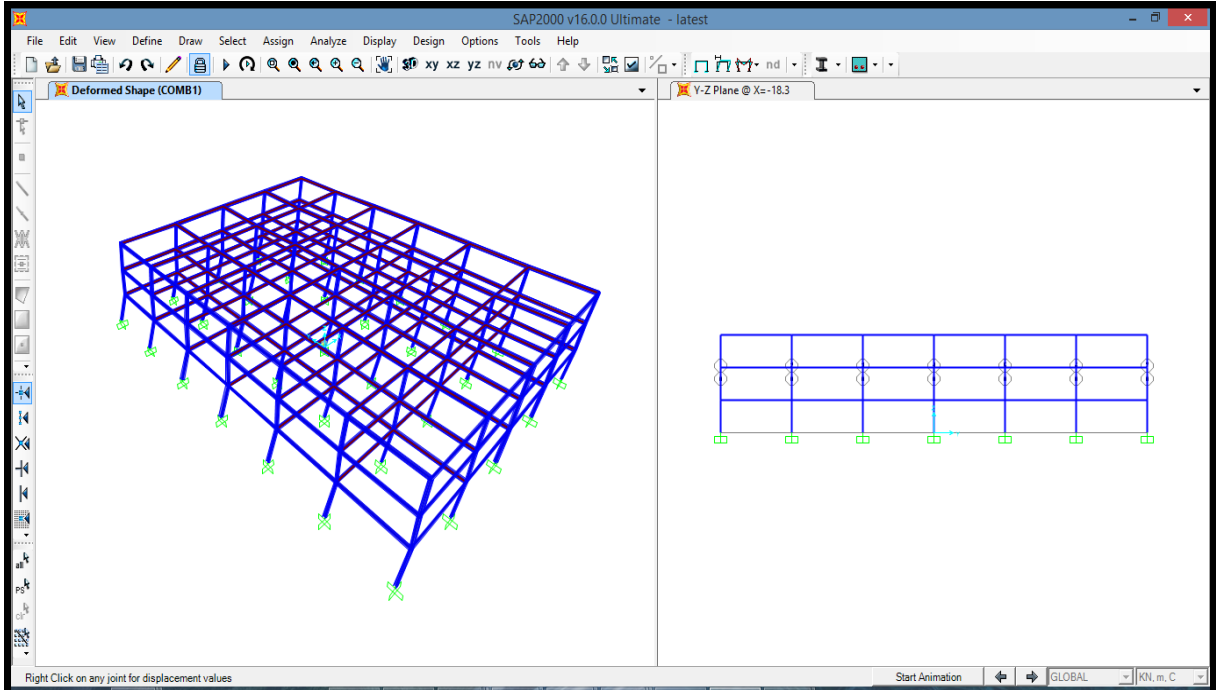


Figure 7.5 The behaviour of full structure, under the combination of the DL+LL+ Time History Loading

b. The behaviour of one of the face:

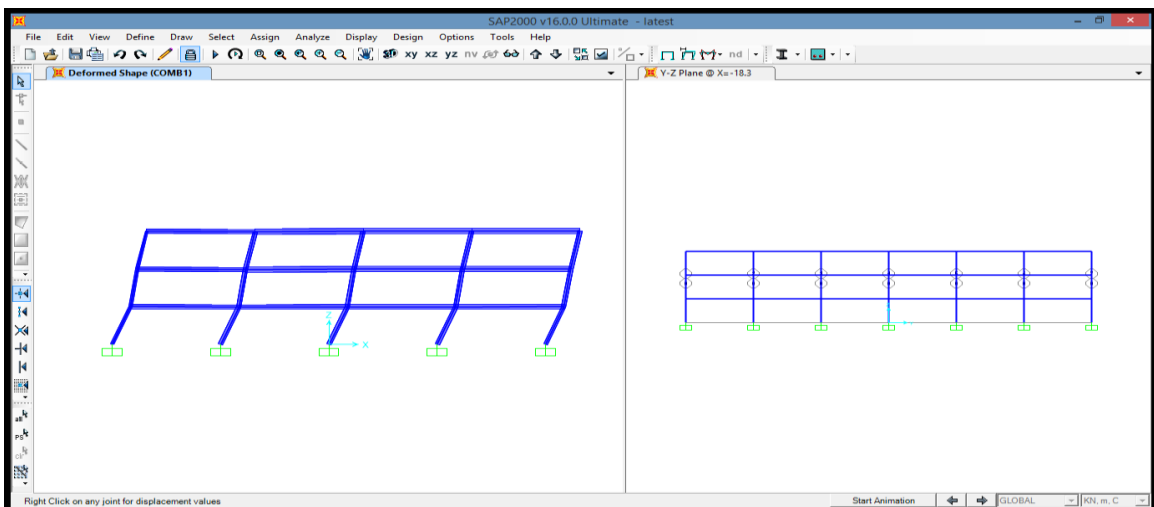


Figure 7.6 The behavior of the one of the faces, under the combination of the DL+LL+ Time History Loading

c. The display plot function of joint C4:

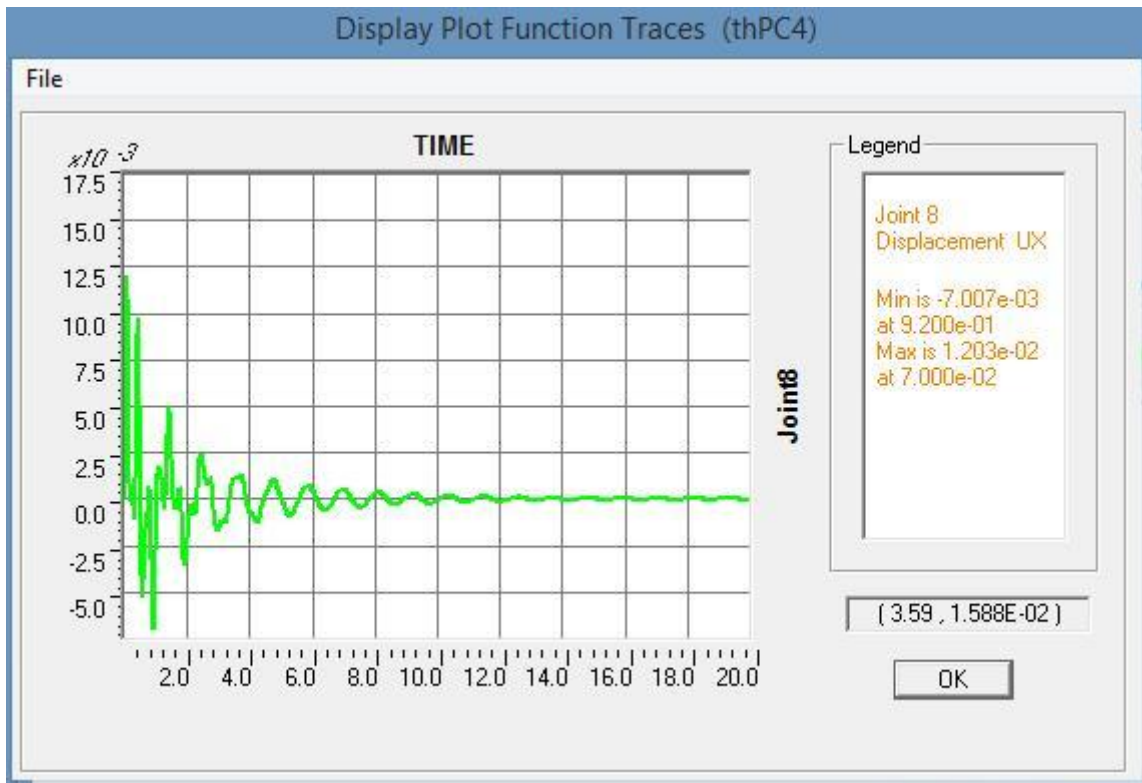


Figure 7.7 The display plot function of joint C4

Estimation of Probability of Failure

8.1. Probability of Failure for different values of the Charge Weight (W)

8.1.1. Visual Basic Application for MS-Excel

Excel VBA (Visual Basic for Applications) is the name of the programming language of Excel.

Visual Basic for Applications enables building user-defined functions (UDFs) and automating processes. VBA code normally can only run within a host application, rather than as a standalone program. VBA can, however, control one application from another using OLE Automation. For example, VBA can automatically create a Microsoft Word report from Microsoft Excel data that Excel collects automatically from polled sensors. Similarly, the VBA has been used to run automatic analysis on SAP2000 from MS Excel, thus forming a SAP-VBA interface.

8.1.2. Sensitivity Analysis

Before performing probabilistic analysis, sensitivity analysis should be done to find out how much the responses are sensitive to design and applied load parameters. Three different methods to perform sensitivity analysis are used:

First Order Second Moment (FOSM) method,

-Monte Carlo Simulation (MCS) and

-Tornado Diagrams (TD).

Here we have employed Monte Carlo Simulation (MCS) to carry out the sensitivity analysis.

8.1.3. Monte Carlo Simulation (MCS)

Sensitivity analysis may also be performed by MCS method (Shudler, 1997). In this method, it is necessary to know the probability density function of all random variables at the beginning of process. For large number of variables, MCS is more convenient (Bucher, 1988). MCS method can be used to verify other proposed methods (Lee and Mosalam, 2006). In MCS, random variables should be generated with their mean and standard deviation.

Monte Carlo simulation performs risk analysis by building models of possible results by substituting a range of values—a probability distribution—for any factor that has inherent uncertainty. It then calculates results over and over, each time using a different set of random values from the probability functions. Depending upon the number of uncertainties and the ranges specified for them, a Monte Carlo simulation could involve thousands or tens of thousands of recalculations before it is complete. Monte Carlo simulation produces distributions of possible outcome values.

By using probability distributions, variables can have different probabilities of different outcomes occurring. Probability distributions are a much more realistic way of describing uncertainty in variables of a risk analysis. The Normal probability distributions have been used.

Normal – Or “bell curve.” The user simply defines the mean or expected value and a standard deviation to describe the variation about the mean. Values in the middle near the mean are most likely to occur. It is symmetric and describes many natural phenomena.

8.1.4. Procedure to Find the Probability of Failure

STEP I

To find the values of blast load (in kN) for different values of charge weight (W). The values of blast load have been found at each joint of the face of the building keeping the radial distance constant at 5m.

The different values of charge weight used are 5 kg, 10 kg, 20 kg, 30 kg, 40 kg, 50 kg, 60 kg, 70 kg, 80 kg, 90 kg, 100 kg, 110 kg, 120 kg, 130 kg, 140 kg and 150 kg.

The .Excel sheets showing the calculated values of blast load have been attached.

STEP II

A program has been developed in MS Excel using the VBA or Visual Basic for Applications. This program has been developed in such a way that it incorporates the SAP2000 file.

STEP III

Using the above program we will get the probability of failure of the building. The probability of failure for Face I and Face II of the building have been calculated at a standoff distance of 5m

The figure showing the different faces of the building are as follow:

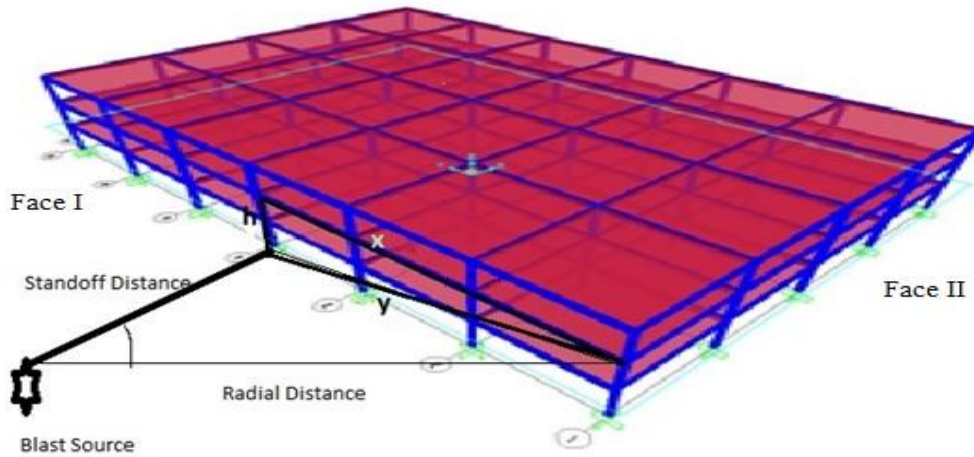


Figure 8.1 Different faces of building

The same program is used to calculate the probability of failure of the building for different values of charge weight between 5kg and 150kg. Using the findings of the program we can plot the graph for the Probability of failure (Pf) vs. Charge Weight keeping the standoff distance constant at 5m.

The Pf vs. Charge Weight (kg) is as follow :

1. Face I of the building-

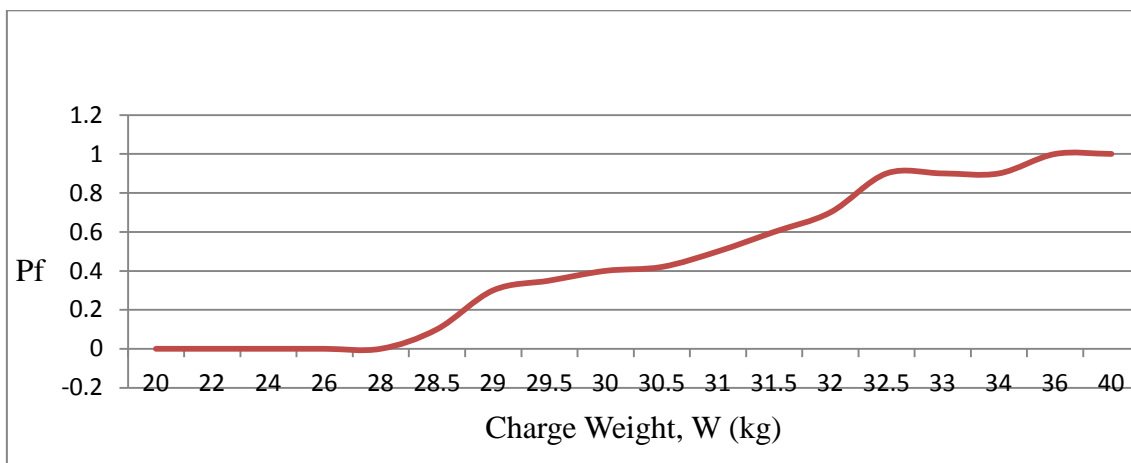


Figure 8.2 Pf vs. Charge Weight (kg) for Face I

2. Face II of the building-

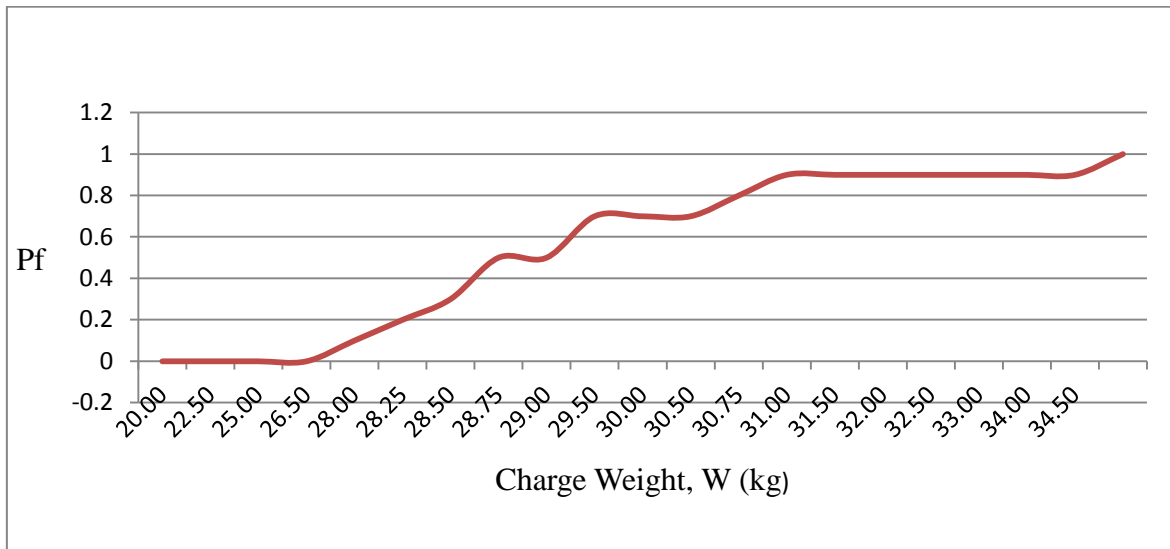


Figure 8.3 Pf vs. Charge Weight (kg) for Face II

8.2. Probability of failure for different values of the Charge Weight (W) keeping the Standoff Distance constant at 10 m.

Similarly, the plots for the standoff distance of 10 m have been plotted. These are as follow:

1. Face I of the building-

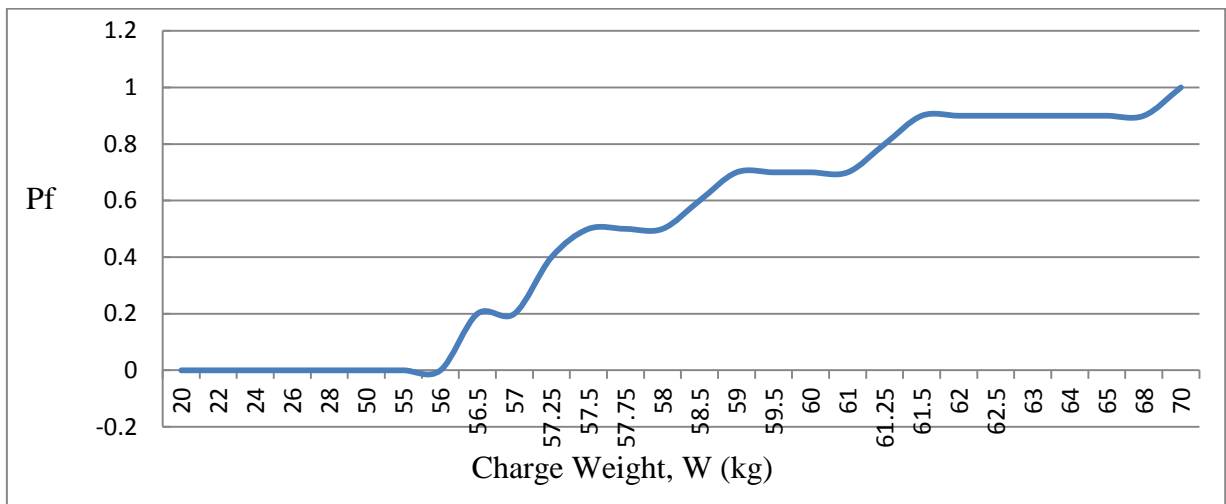


Figure 8.4 Pf vs. Charge Weight (kg) for Face I

2. Face II of the building-

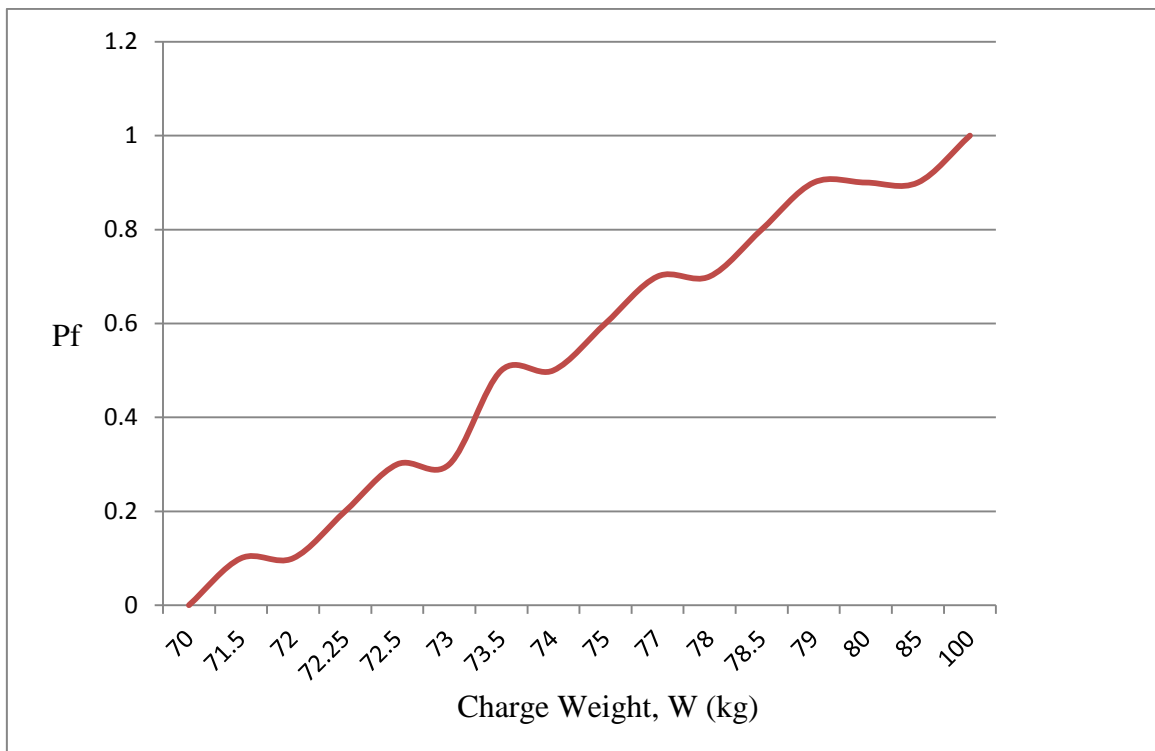


Figure 8.5 Pf vs. Charge Weight (kg) for Face II

8.3. Interpretation of Results

1. For standoff distance of 5 m from the face of the building-

- The face I of the building does not fail for all the charge weights below 28 kg while the building completely fails for all the charge weight above 40kg.
- The face II of the building does not fail for charge weights below 26.5 kg, while the failure of the building occurs for all weights above 35 kg.

2. For standoff distance of 10 m from the face of the building-

- The face I of the building does not fail for all the charge weights below 56 kg, while the failure occurs for all the charge weights above 70 kg.
- The face II of the building does not fail for all charge weights below 70 kg, while the failure occurs for all the charge weights 85 kg.

Conclusions

9.1. Conclusions

It is observed from literature survey that for the estimation of blast load or pressure the empirical approach (Kinney and Graham's) proves to be ideal as otherwise the blast phenomenon is complex in nature. Complexity arises due to unpredictability of charge weight and standoff distance, the behaviour of material under different loading conditions and post blast triggering events.

A three storey steel building was subjected to blast load under varying conditions like different charge weights and standoff distances of 5 m and 10 m respectively.

The following observations and conclusions can be drawn from the present study.

1. The value of peak reflected pressure as evident from the plots is very high for the radial distance up to 10 m and there is a significant drop (about 2-3 times) in the values of the peak reflected pressure from 10 m to 20 m.
2. Also, the values of the peak reflected pressure, for all charge weights, is low for all the radial distances beyond 20 m. Peak reflected pressure increases about 4 times when angle of incidence decreases from 90° to about 0° .
3. This implies that the parking lots should not be constructed in front of the face of the building and a minimum distance from the face of the building should be 10 m, to avoid damage to building due to vehicle bombs.
4. The parking lots should always be constructed at the corners, such that the angle of incidence of the blast load to the main structural frame of the building always remains higher. Keeping the angle of incidence values high causes the blast load to be reduced significantly.
5. The parking lots should never be constructed near the entrant corners of the building as the radial distance to the entrant corner of the building may be less than 10 m and the values of the angle of incidence will be high for the same scenario and shock wave reflections may causes significant damage
6. For the face I of the building the coefficient of variation for charge weight is 0.144 while that for the moment is 0.131. This implies that the effect of uncertainty in the

values of the charge weight does not magnify the effect of uncertainty in the values of bending moments.

7. Similarly, for the face II of the building the coefficient of variation for charge weight is 0.144 while that for moment is 0.128. This implies that the effect of uncertainty in the values of the charge weight does not magnify the effect of uncertainty in the values of bending moments.
8. Since the values of the skewness and kurtosis are similar in both the cases so there is no significant variation in terms of these quantities.
9. For standoff distance of 5 m from the face of the building-
 - a. The face I of the building does not fail for all the charge weights below 28 kg while the building completely fails for all the charge weight above 40 kg.
 - b. The face II of the building does not fail for charge weights below 26.5 kg, while the failure of the building occurs for all weights above 35 kg.
10. For standoff distance of 10 m from the face of the building-
 - a. The face I of the building does not fail for all the charge weights below 56 kg, while the failure occurs for all the charge weights above 70 kg.
 - b. The face II of the building does not fail for all charge weights below 70 kg, while the failure occurs for all the charge weights 85 kg.

9.2. Scope of Further Work

The following may be considered for the possible extension to the work presented herein.

1. Verification of pressure computation done by Kinney Graham's approach by JWL approach using any FEM program such as ABAQUS, Autodyn or LS-Dyna.
2. The reliability analysis of the structure can be carried out by forming the fragility curves for the following scenario:
 - a. Curve between Probability of failure and Radial Distance (R) for different values of the Charge Weight (W).
 - b. Fragility of the frames may also be obtained for uncertain standoff distances.

REFERENCES

1. Brian R. I., Sezen, H., (2013). “Experimental and analytical progressive collapse assessment of a steel frame building.” *Engineering Structures* 56 664–672.
2. Dewey, M.C., Dewey J.M., (1971), “The properties of the blast waves obtained from the particle trajectories”, *Proc. R. Soc. Lond. A.314*, pp. 275-299.
3. Dharaneepathy M. V. (1995), “Critical distance for blast resistance design”, *computer and structure Vol. 54, No.4*,pp.587-595.
4. Fang F. (2009)., “Progressive collapse analysis of high-rise building with 3-D finite element modelling method.” *Journal of Constructional Steel Research* 65- 1269-1278.
5. Jinkoo. K., Park, J. H., Lee, T. H., (2010). “Sensitivity analysis of steel buildings subjected to column loss.” *Engineering Structures* 33 421–432.
6. Khadid M., Zhou, F.,(2006) “The fully fixed stiffened plates under the effect of blast loads”, *Journal of Structural Engineering, ASCE*.
7. Mark. C. A., Archilla, J. C., (2006). “A Model for Progressive Collapse of Conventional Framed Buildings.” *17th analysis and computation specialty conference*.
8. Mehrdad S., Kazemi, A., Sagiroglu, S., Forest, S. (2011). “Progressive Collapse Resistance of an Actual 11-Story Structure Subjected to Severe Initial Damage.” *Journal of Structural Engineering* © ASCE, 893.
9. Nassar, A. A., Razaqpur, A. G., Tait, M. J., Campidelli, M., Foo, S., (2012). “Strength and stability of steel beam columns under blast load.” *International Journal of Impact Engineering* 55 34e48.
10. Nassar, A. A., Razaqpur, A. G., Tait, M. J., Campidelli, M., Foo, S., (2014). “Dynamic Response of Steel Columns Subjected to Blast Loading.” *ASCE*.
11. Ngo, T., Mendis, P.(2007), “Blast Loads and effects of Blast loads on structures”, *EJSE Special Issue: Loading on structures*.
12. Peirs, J., Verleysen, P., Paepegem, W. V., Degrieck, J., (2011). “Determining the stress-strain behaviour at large strains from high strain rate tensile and shear experiments.” *International Journal of Impact Engineering* 38 406e415.
13. Remennikov M. A., (2003) “A review of methods for predicting bomb blast effects on buildings”, *Journal of battlefield technology, vol 6, no 3. pp 155-161*.

14. Ronald. L. S., (2006), “Response of wide flange steel columns subjected to constant axial load and lateral blast load”. *Civil Engineering Department, Blacksburg, Virginia*.
15. Stefan S., Krauthammer, T., (2012). “Energy flow in progressive collapse of steel framed buildings.” *Engineering Structures* 42 142–153.
16. Taewan K., Kim, J., Park, J., (2009). “Investigation of Progressive Collapse-Resisting Capability of Steel Moment Frames Using Push-Down Analysis.” *journal of Performance of constructed facilities* © ASCE, 327.
17. Tavakoli, H. R., Kiakojouri, F. (2013). “Influence of Sudden Column Loss on Dynamic Response of Steel Moment Frames under Blast Loading.” *International Journal of Engineering*.
18. Vlassis, A. G., Izzuddin, B. A., Elghazouli, A. Y., Nethercot, D. A., (2007). “Progressive collapse of multi-storey buildings due to sudden column loss—Part II: Application.” , *Engineering Structures* 30 1424–1438.
19. Wibowo, H., Lau D.T., (2009). “Seismic Progressive Collapse: Qualitative Point of View.” *Civil Engineering Dimension, Vol. 11, No. 1*.
20. Xuemei W., Shi, J., (2013). “Validation of Johnson-Cook plasticity and damage model using impact experiment.” *International Journal of Impact Engineering* 60 67e75.
21. Young. S. H., Anderson, J. C., (2008)., “Response of a Low Rise Steel Building to Air Blast.” *ASCE*.

APPENDIX-A
Computation Sheet for R(m) and Alpha for Standoff Distance 5 m

S.No.	Co-ordinates of point in front of blast at base of the building			Co-ordinates of point vertically above & per. To target point			Co-ordinates of target point			Standoff Distance	<i>h</i>	<i>x</i>	<i>y</i>	<i>R</i>	Alpha
	<i>x</i> ₁	<i>y</i> ₁	<i>z</i> ₁	<i>x</i> ₂	<i>y</i> ₂	<i>z</i> ₂	<i>x'</i> ₂	<i>y'</i> ₂	<i>z'</i> ₂	S.D.					
1	0	0	5	0	11.88	5	27.45	11.88	5	5	11.88	27.45	29.91	30.33	80.51
2	0.00	0.00	5.00	0.00	11.88	5.00	18.30	11.88	5.00	5.00	11.88	18.30	21.82	22.38	77.09
3	0.00	0.00	5.00	0.00	11.88	5.00	9.15	11.88	5.00	5.00	11.88	9.15	15.00	15.81	71.56
4	0.00	0.00	5.00	0.00	11.88	5.00	0.00	11.88	5.00	5.00	11.88	0.00	11.88	12.89	67.17
5	0.00	0.00	5.00	0.00	7.92	5.00	27.45	7.92	5.00	5.00	7.92	27.45	28.57	29.00	80.07
6	0.00	0.00	5.00	0.00	7.92	5.00	18.30	7.92	5.00	5.00	7.92	18.30	19.94	20.56	75.92
7	0.00	0.00	5.00	0.00	7.92	5.00	9.15	7.92	5.00	5.00	7.92	9.15	12.10	13.09	67.55
8	0.00	0.00	5.00	0.00	7.92	5.00	0.00	7.92	5.00	5.00	7.92	0.00	7.92	9.37	57.73
9	0.00	0.00	5.00	0.00	3.96	5.00	27.45	3.96	5.00	5.00	3.96	27.45	27.73	28.18	79.78
10	0.00	0.00	5.00	0.00	3.96	5.00	18.30	3.96	5.00	5.00	3.96	18.30	18.72	19.38	75.05
11	0.00	0.00	5.00	0.00	3.96	5.00	9.15	3.96	5.00	5.00	3.96	9.15	9.97	11.15	63.37
12	0.00	0.00	5.00	0.00	3.96	5.00	0.00	3.96	5.00	5.00	3.96	0.00	3.96	6.38	38.38
13	0.00	0.00	5.00	0.00	0	5.00	27.45	0	5.00	5.00	0.00	27.45	27.45	27.90	79.68
14	0.00	0.00	5.00	0.00	0	5.00	18.30	0	5.00	5.00	0.00	18.30	18.30	18.97	74.72
15	0.00	0.00	5.00	0.00	0	5.00	9.15	0	5.00	5.00	0.00	9.15	9.15	10.43	61.34
16	0.00	0.00	5.00	0.00	0	5.00	0.00	0	5.00	5.00	0.00	0.00	0.00	5.00	0.00

APPENDIX-A

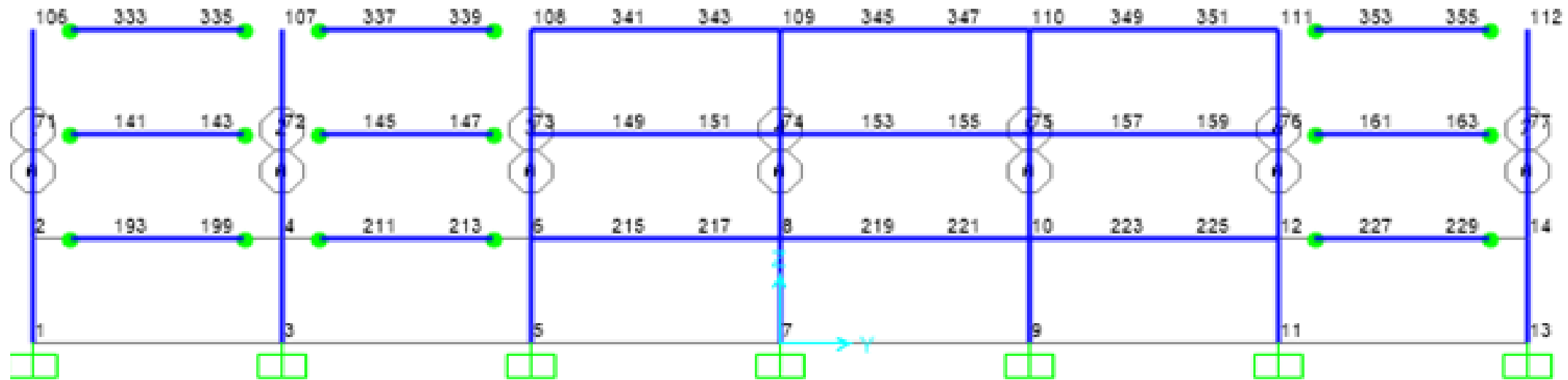
Computation Sheet for R(m) and Alpha for Standoff Distance 10 m

S.No.	Co-ordinates of point in front of blast at base of the building			Co-ordinates of point vertically above & per. To target point			Co-ordinates of target point			Standoff Distance	<i>h</i>	<i>x</i>	<i>y</i>	<i>R</i>	Alpha
	<i>x</i> ₁	<i>y</i> ₁	<i>z</i> ₁	<i>x</i> ₂	<i>y</i> ₂	<i>z</i> ₂	<i>x'</i> ₂	<i>y'</i> ₂	<i>z'</i> ₂	S.D.					
1	0	0	10	0	11.88	10	27.45	11.88	10	10	11.88	27.45	29.91	31.54	71.51
2	0.00	0.00	10.00	0.00	11.88	10.00	18.30	11.88	10.00	10.00	11.88	18.30	21.82	24.00	65.37
3	0.00	0.00	10.00	0.00	11.88	10.00	9.15	11.88	10.00	10.00	11.88	9.15	15.00	18.02	56.30
4	0.00	0.00	10.00	0.00	11.88	10.00	0.00	11.88	10.00	10.00	11.88	0.00	11.88	15.53	49.91
5	0.00	0.00	10.00	0.00	7.92	10.00	27.45	7.92	10.00	10.00	7.92	27.45	28.57	30.27	70.71
6	0.00	0.00	10.00	0.00	7.92	10.00	18.30	7.92	10.00	10.00	7.92	18.30	19.94	22.31	63.37
7	0.00	0.00	10.00	0.00	7.92	10.00	9.15	7.92	10.00	10.00	7.92	9.15	12.10	15.70	50.43
8	0.00	0.00	10.00	0.00	7.92	10.00	0.00	7.92	10.00	10.00	7.92	0.00	7.92	12.76	38.38
9	0.00	0.00	10.00	0.00	3.96	10.00	27.45	3.96	10.00	10.00	3.96	27.45	27.73	29.48	70.17
10	0.00	0.00	10.00	0.00	3.96	10.00	18.30	3.96	10.00	10.00	3.96	18.30	18.72	21.23	61.89
11	0.00	0.00	10.00	0.00	3.96	10.00	9.15	3.96	10.00	10.00	3.96	9.15	9.97	14.12	44.91
12	0.00	0.00	10.00	0.00	3.96	10.00	0.00	3.96	10.00	10.00	3.96	0.00	3.96	10.76	21.60
13	0.00	0.00	10.00	0.00	0	10.00	27.45	0	10.00	10.00	0.00	27.45	27.45	29.21	69.98
14	0.00	0.00	10.00	0.00	0	10.00	18.30	0	10.00	10.00	0.00	18.30	18.30	20.85	61.34
15	0.00	0.00	10.00	0.00	0	10.00	9.15	0	10.00	10.00	0.00	9.15	9.15	13.55	42.46
16	0.00	0.00	10.00	0.00	0	10.00	0.00	0	10.00	10.00	0.00	0.00	0.00	10.00	0.00

APPENDIX- B

Blast Pressure Calculation Sheet for Standoff Distance 5 m

Joint No.	R(m)	α°	TNT (kg) \rightarrow	5.00	10.00	20.00	30.00	40.00	50.00	60.00	70.00	80.00	90.00	100.00	110.00	120.00	130.00	140.00	150.00
8.00	10.76	21.60	Pref	118.18	187.85	415.24	619.86	823.19	1021.92	1223.16	1415.69	1602.59	1788.16	1971.99	2151.57	2337.21	2518.25	2700.07	2882.80
74.00	12.76	38.38	kN/m ² \downarrow	55.58	103.02	106.57	132.24	158.72	230.07	203.68	278.78	300.45	318.99	336.14	353.35	373.45	414.59	441.76	479.79
109.00	15.53	49.91		38.91	52.45	68.42	82.91	95.15	105.24	113.14	122.74	133.68	144.04	154.83	164.23	173.15	182.80	190.92	198.63
6.00	14.12	44.91		54.37	72.02	92.40	112.04	122.36	143.06	160.02	176.49	191.79	206.04	217.95	240.23	247.63	261.76	276.68	290.58
73.00	15.70	50.43		38.61	51.33	66.49	80.43	82.06	103.02	96.03	119.41	130.02	140.06	150.51	159.62	188.52	176.51	185.52	193.00
108.00	18.02	56.30		27.34	33.73	44.30	51.05	54.95	62.60	69.71	75.89	82.10	89.11	94.12	99.41	104.41	109.90	115.21	120.37
4.00	21.23	61.89		19.28	23.73	29.84	35.57	40.61	45.19	48.95	52.55	56.11	59.76	63.20	66.88	69.97	73.39	76.18	79.36
72.00	22.31	63.37		17.91	21.06	27.29	46.99	37.79	41.45	45.32	48.26	51.44	54.02	57.41	60.66	63.40	66.42	68.89	71.69
107.00	24.00	65.37		14.75	18.45	21.80	26.14	30.00	33.03	36.13	38.99	42.18	45.28	46.14	48.30	50.68	53.34	55.19	57.32
2.00	29.48	70.17		8.17	12.16	15.74	17.95	19.89	22.88	23.50	25.77	27.29	29.07	30.59	32.04	33.43	34.76	36.03	37.26
71.00	30.27	70.71		7.91	11.89	15.17	17.91	19.71	21.93	23.25	25.14	26.94	27.75	29.18	30.75	32.06	33.31	34.75	35.43
106.00	31.54	71.51		7.52	11.85	14.33	16.87	18.51	20.55	21.75	23.48	25.12	26.70	27.50	28.75	30.05	31.09	32.41	33.70



APPENDIX- B
Blast Pressure Calculation Sheet for Standoff Distance 10 m

Joint No.	R(m)	α°	TNT (kg)→	5	10	20	30	40	50	60	70	80	90	100	110	120	130	140	150
8	10.76	21.60	Pref	41.14107	63.14548	104.4927	146.1077	209.2316	251.8336	294.448	337.2237	380.2483	423.5759	500.0666	545.2428	590.5848	636.1122	681.839	727.7756
74	12.76	38.38	(in kN/m ²)	31.05443	45.76158	71.35466	96.14327	120.9614	145.9795	171.3475	228.3478	256.3304	284.4915	312.8627	341.465	370.3128	399.4156	428.7799	458.4098
109	15.53	49.91	↓	24.78231	36.52146	56.98647	76.6852	96.43157	111.9171	126.909	141.5392	155.8918	170.0241	183.9772	197.7818	179.5451	188.1358	196.3643	204.2502
6	14.12	44.91	↓	27.41136	39.83273	61.21019	81.1753	102.7996	124.905	147.6011	170.9372	194.9352	220.0645	238.1516	255.9865	273.6004	291.0183	308.2603	325.3434
73	15.70	50.43	↓	24.51197	36.181	56.27848	75.56597	94.90735	110.2189	124.4043	138.1382	151.5101	164.5815	177.3972	189.9908	172.626	180.8715	188.7714	196.3446
108	18.02	56.30		20.8184	31.48031	47.22335	60.54223	73.22668	85.61412	97.86542	106.5377	113.5094	119.869	125.6733	130.9662	135.7826	140.151	144.0955	147.6363
4	21.23	61.89		17.34646	25.38329	39.28468	47.17582	53.92921	59.92785	65.36283	70.34604	74.94985	79.2245	83.20669	87.16556	90.96326	94.5631	97.97854	101.2208
72	22.31	63.37		16.71146	23.99963	36.33904	44.62605	50.60246	55.82747	60.48981	64.69995	68.52937	72.02769	75.23117	78.16734	80.99632	84.28904	87.43438	90.44205
107	24.00	65.37		15.17903	22.26422	32.27979	40.75191	45.87881	50.31023	54.22449	57.72566	60.88091	63.73672	66.32695	68.67723	70.80764	72.73423	74.4702	76.32461
2	29.48	70.17		11.55903	19.67488	25.24201	28.26574	30.39789	31.9368	34.04822	36.35741	38.49877	40.50046	42.38272	44.16065	45.84591	47.44771	48.97349	50.42935
71	30.27	70.71		10.60466	17.99106	24.0339	26.99563	29.13166	30.72351	32.24277	34.43049	36.46249	38.36545	40.15849	41.85589	43.46865	45.00544	46.47327	47.87788